

Design and Evaluation of Hybrid Energy Storage Systems for Electric Powertrains

by

Karl BA. Mikkelsen

A thesis

presented to the University of Waterloo

in fulfillment of the

thesis requirement for the degree of

Master of Applied Science

in

Mechanical Engineering

Waterloo, Ontario, Canada, 2010

© Karl BA. Mikkelsen 2010

Author's Declaration

I hereby declare that I am the sole author of this thesis. This is a true copy of the thesis, including any required final revisions, as accepted by my examiners.

I understand that my thesis may be made electronically available to the public.

Abstract

At the time of this writing, increasing pressure for fuel efficient passenger vehicles has prompted automotive manufactures to invest in the research and development of electrically propelled vehicles. This includes vehicles of strictly electric drive and hybrid electric vehicles with internal combustion engines.

To investigate some of the many technological innovations possible with electric power trains, the AUTO21 network of centres of excellence funded project E301-EHV; a project to convert a Chrysler Pacifica into a hybrid electric vehicle. The converted vehicle is intended for use as a test-bed in the research and development of a variety of advances pertaining to electric propulsion. Among these advances is hybrid energy storage, the focus of this investigation.

A key difficulty of electric propulsion is the portable storage or provision of electricity, challenges are twofold; (1) achieving sufficient energy capacity for long distance driving and (2) ample power delivery to sustain peak driving demands. Where gasoline is highly energy dense and may be burned at nearly any rate, storing large quantities of electrical energy and supplying it at high rate prove difficult. Furthermore, the demands of regenerative braking require the storage system to undergo frequent current reversals, reducing the service life of some electric storage systems.

A given device may be optimized for one of either energy storage or power delivery, at the sacrifice of the other. A hybrid energy storage system (HESS) attempts to address the storage needs of electric vehicles by combining two of the most popular storage technologies; lithium ion batteries, ideal for high energy capacity, and ultracapacitors, ideal for high power discharge and frequent cycles.

Two types of HESS are investigated in this study; one using energy-dense lithium ion batteries paired with ultracapacitors and the other using energy-dense lithium ion batteries paired with ultra high powered batteries. These two systems are compared against a control system using only batteries. Three sizes of each system are specified with equal volume in each size. They are compared for energy storage, energy efficiency, vehicle range, mass and relative demand fluctuation when simulated for powering a model Pacifica through each of five different drive cycles.

It is shown that both types of HESS reduce vehicle mass and demand fluctuation compared to the control. Both systems have reduced energy efficiency. In spite of this, a battery-battery system increases range with greater storage capacity, but battery-capacitor systems have reduced range.

It is suggested that further work be conducted to both optimize the design of the hybrid storage systems, and improve the control scheme allocating power demand across the two energy sources.

Acknowledgements

For his support, astute guidance and unfaltering patience, I would like to thank my supervisor; Professor Stephan Blair Lambert of the faculty of Mechanical and Mechatronics Engineering at the University of Waterloo. I would like to extend a debt of gratitude to a host of researchers for sharing their collective wealth of knowledge with me. These include Dr. Salama and Dr. Kazerani of the faculty of Electrical and Computer Engineering at the University of Waterloo, Dr. Rideout of Memorial University of Newfoundland, Dr. Minaker of the University of Windsor, and Dr. Rohraur of the University of Ontario Institute of Technology. I would especially like to thank Dr. Rohraur's student, Pierre Hinse, for inspiring my interest in electric drive trains.

This study would not have been possible without the continued financial support of AUTO21, a network of centres of excellence promoting academic research in the automotive industry within Canada. By extension, I thank AUTO21's benefactors, the Natural Sciences and Engineering Research Council of Canada.

I also wish to thank my family. The perpetual encouragement, wisdom, and understanding they have shown me has been of immense value.

Dedication

I dedicate this thesis to my friend Arija. Thank you for always helping me find joy in whichever moment I'm living in.

Table of Contents

Author's Declaration	ii
Abstract	iii
Acknowledgements	v
Dedication	vi
Table of Contents	vii
List of Tables	x
List of Figures	xi
1.0 Introduction	1
1.1 Motivation for Electrified Vehicles	2
1.2 Background to Electrified Vehicles	3
1.3 Pacifica Background	4
1.4 Thesis Objectives	5
2.0 Literature Review	6
2.1 Vehicle Power Requirements	6
2.2 EV Powertrain Technologies	9
2.2.1 Transmission and Running Gear	9
2.2.2 Electric Motors	10
2.2.3 Inverters	12
2.2.4 DC/DC Converters	13
2.3 EV Storage Technologies	14
2.3.1 Batteries	14
2.3.2 Ultra capacitors	19
2.3.3 Comparison of Storage Technologies	21
2.3.4 Hybrid Energy Storage	23
2.3.5 Hybrid Control and Power Management	25
2.4 Powertrain Evaluation	26
3.0 Vehicle Configuration and Simulation	29
3.1 Vehicle Configuration	29
3.1.1 Powertrain	30

3.1.2	Hybrid Energy Storage Design Strategy	32
3.2	Simulation Structure	35
3.2.1	Overview	35
3.2.2	Inputs	37
3.2.3	Vehicle Drag Force	38
3.2.4	Running power	39
3.2.5	Motor	40
3.2.6	Inverter	42
3.2.7	DC Converter	43
3.2.8	HESS	47
3.3	Validation	49
4.0	Results	50
4.1	Scenarios	50
4.1.1	Energy Storage Systems	50
4.1.2	Drive Schedules	51
4.1.3	Simulation Matrix	52
4.2	Results	52
4.2.1	Range and Energy Efficiency Estimation	52
4.2.2	Service Life Effects	59
4.2.3	Implications	61
4.3	Limitations	63
4.3.1	Simplification and Approximation	63
4.3.2	Drive Schedule	64
4.3.3	Hybrid Control Scheme	64
4.3.4	Battery Service Life	65
4.3.5	Chapter Summary	65
5.0	Conclusions and Recommendations	66
5.1	Conclusions	66
5.2	Recommendations	67
References		69

Appendices

Appendix A - Chrysler Pacifica Specifications	74
Appendix B - Gapped Inductor Design for DC-DC Converter	78
Appendix C - Battery Discharge Model	84
Appendix D - Battery and Capacitor Cell Parameters	85
Appendix E - Energy Usage Graphs	87
Appendix F - Demand Variation Graphs	90

List of Tables

Table 1.1 - Pacifica specifications	4
Table 2.1 - Drive cycle statistics	7
Table 2.2 - Battery cell comparison (Masrur and Mi 2006)	18
Table 2.3 - Comparison of storage and conversion technologies	21
Table 3.1 - Power system properties	34
Table 4.1 - Energy storage systems under consideration for Pacifica conversion	51
Table 4.2 - Simulation matrix	52

List of Figures

Figure 1.A - Parallel vs. series hybrid configurations	4
Figure 1.B - Proposed drive train topology for the Pacifica	5
Figure 2.A - Motor torque and power vs. shaft speed	11
Figure 2.B - Li-ion battery schematic	15
Figure 2.C - Cell chemistry specific energy vs. specific power, gravimetric	19
Figure 2.D - Capacitor and ultracapacitor schematic	20
Figure 2.E - Energy density vs. power density, volumetric	23
Figure 2.F - Battery-capacitor coupling options	25
Figure 3.A - Powertrain overview	31
Figure 3.B - Powertrain calculation procedure	36
Figure 3.C - System overview	37
Figure 3.D - Drive cycle input	38
Figure 3.E - Drag force schematic	39
Figure 3.F - Running power schematic	40
Figure 3.G - Motor schematic	42
Figure 3.H - Inverter schematic	43
Figure 3.I - DC-DC converter schematic	44
Figure 3.J - Energy management system schematic	45
Figure 3.K - DC-DC converter loss schematic	46
Figure 3.L - HESS calculations	48
Figure 4.A - Range vs. storage system mass	53
Figure 4.B - Range vs. mass per drive schedule	55
Figure 4.C - Energy usage breakdown for UDDS	57
Figure 4.D - Energy usage breakdown for US06	58
Figure 4.E - Normalized current demand for US06	59
Figure 4.F - Normalized current demand for UDDS	60

1.0 Introduction

As of 2010, the most prominent aspect for improvement required of the automotive industry is clear: governments and consumers are increasingly demanding vehicles with better fuel efficiency and lower emissions. This demand began in the early 1970's with the Arab Oil Embargo (U.S. Dept. of State Office of the Historian) followed by the advent of the United States Corporate Average Fuel Economy (CAFE) regulations in 1975 (National Highway and Traffic Safety Administration, 2010). The trend persisted through the 1990's with the California Air Resources Board (CARB) requiring a fraction of vehicles sold in California to be zero emission vehicles (Westbrook, 2001).

Each manufacturer has responded uniquely to the demand for fuel efficiency; however, a common theme is a move toward electrification of the powertrain. General Motors began with the EV1 in 1996. The EV1 was, for most intents and purposes, the first production electric car since the Baker Electric in 1921 (Westbrook, 2001). GM's most recent research efforts in improving fuel efficiency include two-mode hybrid systems (Sherman, 2009), a gas-electric series hybrid called the 'Volt' (General Motors Canada, 2010), and homogenous charge compression ignition engines (Abuelsamid, 2007). Toyota produced the first mass market parallel hybrid vehicle, the Prius, released in North America in 1997 (Westbrook, 2001). Ford has announced a battery powered version of the Focus to be available in 2011 (Patrascu, 2010).

Interest in fuel efficiency spearheads an accelerating shift toward electrified vehicles that appears to be beginning with partially electric drive trains, like those of gas-electric hybrids, and progressing to completely electric propulsion. This shift presents a host of technical challenges, the most significant of which is the reliable, robust and practical storage of electrical energy for propulsion over long distances. A handful of portable electricity sources exist, such as fuel cells or batteries, with varying benefits and detriments. A major challenge is the balance between sufficient *energy storage* for adequate electric-only range, coupled with sufficient *power capability* for acceleration (and deceleration) performance.

One of many answers to the problems of energy storage is to combine two different storage devices in order to leverage the benefits of each; a hybrid energy storage device. Hybrid electric energy storage poses

a host of technical, design and evaluation requirements, the implications of which are addressed in this work. This section provides background to electrified vehicles, introduces a specific design case, and gives an outline for the content to follow.

1.1 Motivation for Electrified Vehicles

The attractions of electric transportation are many, but the primary incentives stem from the problems of the prevalent alternative: the combustion of fossil fuels. Hydrocarbon combustion is substantially responsible for degraded air quality, especially in densely populated areas, and for human-associated greenhouse gas emissions (Hodkinson, et al., 2001). Internal combustion presently relies directly on the availability of crude oil, the procurement of which is a politically and environmentally sensitive process. Disruptions to the supply of oil result in price swings and economic uncertainty. Additionally, crude oil is in finite supply, and a substantial amount of the original worldwide reserves have already been consumed (Styles, 2010). Automobile ownership is increasing worldwide (Hodkinson, et al., 2001) and the consumption of crude oil is likely to increase at a matching pace. General awareness is growing for the unsustainable nature of fossil fuels, and the need for a viable alternative energy source for transportation.

Generating sources for electricity are numerous, and environmentally benign sources such as wind, solar and hydrostatic generation are finding increasing public favour. The multitude of options for producing electricity reduces the risk of supply disruption. Furthermore, the efficiency of converting stored energy to mechanical energy is on the order of 80% for electric propulsion, compared to internal combustion which is at best 30% (Masrur, et al., 2006). The price of electricity is much less than that of gasoline and also more stable (Paine, 2006).

The benefits of electric transportation are countered by difficulties in storing electrical energy for use in vehicles. Market research indicates that consumers are willing to purchase electric vehicles if performance, range and service life all match or exceed that of traditional gasoline powered vehicles (LeBlanc, 2010) at or below the cost of gasoline cars. Present options for storing electric energy include fuel cells, ultra-capacitors and a variety of battery types, none of which are yet able to compete with gasoline on the aforementioned metrics by themselves.

1.2 Background to Electrified Vehicles

Many types of electrified vehicles exist. They are categorized by energy storage type and by degree of electrification. At one end of the spectrum of electrification is a conventional gasoline powered vehicle and at the other, a fully electrified vehicle. In between the two are hybrid electric vehicles (HEVs). By definition, a hybrid vehicle uses two propulsion methods - for instance gasoline and electric. Depending on the relative power of the electric motor and combustion engine, the vehicle may be termed a 'micro hybrid', 'mild hybrid', or 'full hybrid' (Johnson Controls, 2010). Some hybrids are capable of increased electric operation if their batteries are first charged by an external electricity supply, these are known as plug-in hybrid electric vehicles (PHEV). Fully electric vehicles are categorized according to their power source, for instance battery electric vehicles (BEV), or fuel cell electric vehicles (FCEV). The term electrified vehicle (EV) broadly refers to all of these varieties.

HEVs may use a parallel or series configuration of engine and motor. In a parallel configuration, the engine is mechanically connected to the drive wheels and can operate the car independently. This approach is used by Honda's integrated motor assist topology (Honda Motor Co., Ltd., 2010). In a series hybrid such as the Chevrolet Volt, the engine is used exclusively for generating electricity with which to run the motor (General Motors Canada, 2010). Figure 1.A shows typical configurations for series and parallel hybrid drive trains.

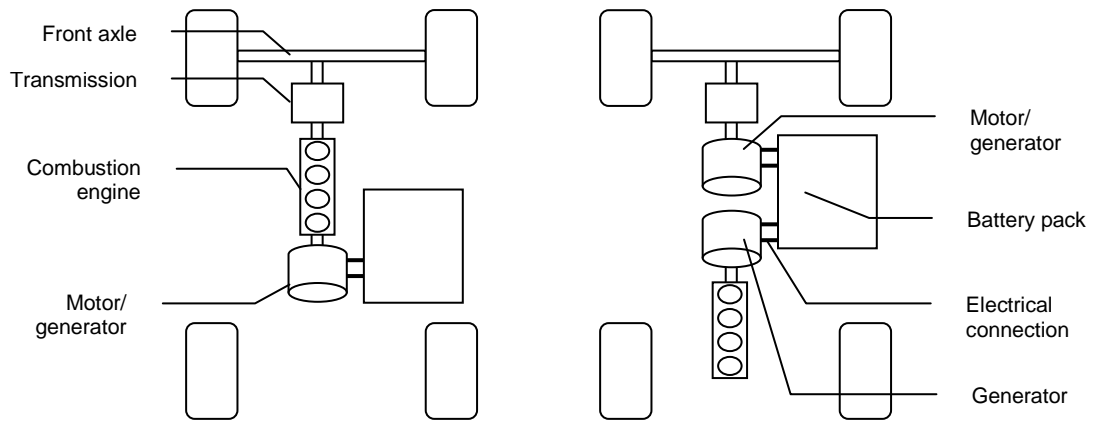


Figure 1.A - Parallel vs. series hybrid configurations

1.3 Pacifica Background

Many advantages related to propulsion and otherwise, can be gained or made easier to implement with a vehicle using an electric drive train. These advantages include torque vectoring, active handling and stability control, intelligent grid interfacing, hybrid energy storage, and more. To evaluate these advantages, a project to convert a Chrysler Pacifica to hybrid electric propulsion was initiated by research members of AUTO21, a network of centres of excellence within Canada. The converted Pacifica is intended for use as a test-bed vehicle for use in the research of EV related technologies.

The Pacifica is a crossover minivan and SUV with a six cylinder engine, front wheel drive and automatic transmission. The model used in this project has the all wheel drive option, with a shaft from the rear wheels connecting to the front differential through a power takeoff unit. Key specifications of the 2004 Pacifica are shown in Table 1.1. Detailed specifications are given in Appendix A (Allpar, 2010).

Table 1.1 - Pacifica specifications

Drive type	All wheel drive (AWD)
Engine	3.5L V6
Torque	250 ft.lb @ 3950 rpm
Power	250 hp @ 6400 rpm
Transmission	4 speed automatic
Fuel economy (city/highway)	17/22 mpg
Curb weight	2121 kg

The proposed configuration of the electrified Pacifica includes adding an electrical energy source, DC/DC converter, traction inverter and electric motor with a single speed transmission. The precise mechanical configuration of the drive train is not yet determined, but it is assumed that electric propulsion will be applied to all four wheels. A topology proposed by Steven Samborsky in 2006 includes electric motors at each axle and a battery-capacitor energy storage system as illustrated in Figure 1.B (Samborsky, 2006).

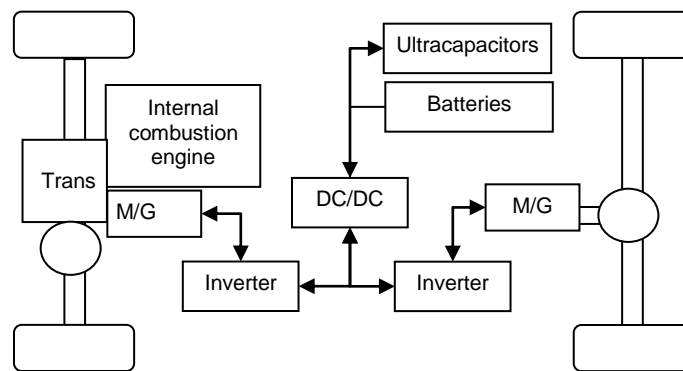


Figure 1.B - Proposed drive train topology for the Pacifica

1.4 Thesis Objectives

The goals of this work are to design a hybrid energy storage system for the Pacifica, and assess its merits over traditional storage solutions. This document begins with a technical review of relevant technologies for energy storage, electric vehicle propulsion and power train evaluation in section 2.0 - Literature Review. The topology (or configuration) of the electric drive train is given for the Pacifica with discussion of the method for evaluation and validation in section 3.0 - Vehicle Configuration and Simulation. The hybrid storage systems to be tested and corresponding test scenarios are presented in section 4.0 - Results. Section 4.0 also includes simulation results and discussion, together with limitations of the evaluation. Conclusions and recommendations are summarized in section 5.0.

2.0 Literature Review

This section summarizes the technical background of electric powertrains and energy usage. It includes an explanation of vehicle running requirements, a brief technical overview of the most common components used in electric drive trains and energy storage systems, and gives consideration to the design of hybrid storage systems and power control schemes. The section concludes with a discussion of overall vehicle powertrain simulation and evaluation.

2.1 Vehicle Power Requirements

Owing to varied speed limits and traffic conditions, a journey by car through a typical city will encounter a wide range of speeds. The journey will also be punctuated by stops due to intersections and other interruptions to traffic such as construction or congestion.

To characterize and measure typical vehicle driving patterns, the United States Environmental Protection Agency (EPA) (United States Environmental Protection Agency 2008) developed a number of drive schedules, or drive cycles, that represent driving conditions expected of a consumer vehicle. The drive schedules consist of a second-by-second record of vehicle velocity. Acceleration and distance may be calculated from the velocity profile, and with details of the vehicle such as mass, coefficient of drag, transmission ratios and efficiency maps, total vehicle power usage can be determined. An important limitation of the drive cycles is that they do not include information about surface incline, and so gravitational running requirements must be neglected.

The drive cycles published by the EPA are used widely in industry as benchmarks for vehicle efficiency and fuel consumption. Among them are the urban dynamic drive schedule (UDDS), the unified drive schedule (LA92), the supplemental federal test procedure (US06), the highway fuel economy driving schedule (HWYCOL) and the New York city schedule (NYCCCOL). More drive cycles exist, though these five cover the widest array of driving situations (United States Environmental Protection Agency 2008).

UDDS is the most used standard drive schedule, represents driving in suburban/city conditions and is regarded as one of the mildest drive cycles published. LA92 was developed by the California Air Resources Board. LA92 also represents city driving but is more aggressive with a higher top speed than UDDS and has considerably higher acceleration. US06 is also city style driving, but is more aggressive than LA92 or UDDS, and includes a greater share of highway travel. HWYCOL includes only a single start/stop with approximately 10 minutes of highway speed travel in between. NYCCCOL reflects travel in dense traffic through a major city centre. Key statistics of all five drive cycles are given in Table 2.1. Note that 30 [m/s] = 108 [km/h].

Table 2.1 - Drive cycle statistics

	UDDS	LA92	US06	NYCCCOL	HWYCOL
Distance [m]	11990	15797	12885	1898	16503
Duration [s]	1369	1435	598	596	765
Average velocity [m/s]	8.8	12.1	21.5	3.2	22.5
Maximum velocity [m/s]	25.3	30.0	35.9	12.4	26.8
Maximum acceleration [m/s²]	1.48	2.82	3.24	2.68	0.94
Minimum acceleration [m/s²]	-1.48	-2.84	-2.82	-2.28	-1.45
Intermediate stops	15	14	4	16	0

Propulsion force requirements, F_p , of a vehicle powertrain are fourfold: (1) rolling resistance, (2) aerodynamic drag, (3) inertial, and (4) gravitational. Propulsion power, P_p is the product of propulsion force and vehicle speed, u .

$$P_p = F_p u \quad (2-i)$$

Gravitational resistance is present only when the vehicle is travelling in the direction of a surface gradient. The sum of forces due to rolling resistance, F_{rr} and aerodynamic drag, F_{ad} make up the total drag. For cruising at constant velocity with no surface gradient, drag is the only propulsion requirement. When accelerating, the force of acceleration, F_{ac} must be added to the drag to give total propulsion requirement.

$$F_p = F_g + F_{rr} + F_{ad} + F_{ac} \quad (2-ii)$$

F_g is proportional to the mass of the vehicle, m , velocity, and the angle of incline, θ .

$$F_g = m g \sin\theta \quad (2\text{-iii})$$

Rolling resistance is a consequence of deformation in the wheels and/or road surface, it is given by

$$F_{rr} = C_r m g \quad (2\text{-iv})$$

where C_r is the coefficient of rolling resistance of the vehicle tires. C_r varies with the type of road surface.

Aerodynamic drag is calculated according to the expression

$$F_{ad} = \frac{1}{2} C_d A \rho u^2 \quad (2\text{-v})$$

where C_d is the drag coefficient corresponding to the vehicle's geometry, A is the frontal surface area, and ρ is the density of air. Finally, the force of acceleration comes from Newton's second law,

$$F_{ac} = m a \quad (2\text{-vi})$$

where a is the instantaneous acceleration of the vehicle. Because F_{ac} is proportional to the vehicle mass and acceleration, it becomes important any time a change in velocity happens, such as accelerating after a stop. It can be shown that for a vehicle travelling through a typical city, F_{ac} is intermittently much higher than drag, and causes F_p to vary widely. F_{ac} becomes negative during deceleration. As a vehicle decelerates, its kinetic energy is reduced, and the difference in kinetic energy at the initial and final velocities is potentially available for recovery.

Various mechanisms are available for the recovery of kinetic energy, including mechanical flywheels and electrical storage. Energy recovered from deceleration may subsequently be used in acceleration, offsetting power demand due to F_{ac} . The amount of kinetic energy available for recovery is significant: for a 1500 [kg] vehicle coming to rest from a highway speed of 100 [km/h], more than 160 [W·hr] may be recovered. For reference, the Chevrolet Volt is expected to have a usable battery capacity of 8 [kW·hr] that is to power the car for 64 [km]. Thus, the recovered energy from each stop from highway speed can extend the range by up to 2%.

Vehicles require power to operate exterior and interior lighting, air conditioning or heating systems, driver instrumentation, etc. This manifests as an accessory load, which varies depending on the equipment used in the vehicle (Miller 2006).

2.2 EV Powertrain Technologies

This section introduces and describes key technologies for devices used in electric powertrains. Focus is given to devices considered for use in the conversion of the Chrysler Pacifica.

2.2.1 Transmission and Running Gear

Many configurations for vehicle running gear exist, with the most common being front wheel drive. Rear wheel, four wheel and all wheel drive are other typical configurations seen on production vehicles; these configurations will typically require a propulsion shaft to transfer torque from the engine, which is usually at the front of the vehicle. Motor/generators can be made much more compact than internal combustion engines, and so electric vehicles have new driveline options available. For instance, multiple motors may be used individually at the front and rear axles, or at each wheel (Editors, Green Car Journal 2010). This brings the benefit of allocating torque selectively to the front or rear, or left to right, known as torque vectoring.

Selection of the drive wheels has importance for regenerative braking. During braking, vehicle weight shifts to the front. To avoid locking the rear wheels, most braking torque must come from the front wheels. It is best to have electric drive at all wheels, but if this is not feasible, it is preferable to have electric drive at the front wheels in order to capture more regenerative braking energy while preserving the normal brake bias.

The torque and efficiency of a combustion engine varies significantly with engine speed, and so most gas engine powered vehicles have a gear box to make the engine's 'torque band' accessible at every driving speed. Some late model vehicles use a continuously variable transmission (CVT) that consist of conical pulleys that can adjust the radius of a connecting belt. As discussed in section 2.2.2 - Electric Motors, electric motors have no need for an adjustable ratio transmission; a single speed reduction is sufficient in most cases.

The modified Pacifica will add an electric motor to both the front and the rear, allowing for regenerative braking from all wheels. A single speed reduction is used for each motor for simplicity.

2.2.2 Electric Motors

Many types of electric motor exist, the simplest being a commutated DC motor, or a brushless AC motor. A host of three-phase motors exist, including synchronous, asynchronous and switched reluctance varieties. The most common choice for electric vehicles is the three phase induction motor. The induction motor finds favour in vehicles because of its high torque and power in a small, light weight package (Westbrook 2001), (Hodkinson and Fenton 2001).

An induction motor has either two or four pairs of windings, or poles, arranged around its stator, for each of the three phases (Westbrook 2001). Supplied with 3 phase alternating current, the windings become magnetically polarized, with the direction of polarization rotating around the shaft of the motor. The rotating magnetic field induces magnetization in the rotor, typically resembling a squirrel cage. The relative speed of the rotor and the rotating magnetic field of the stator induces motion in the rotor. The difference in angular speed between the rotor and the field of the stator is called the slip, which increases with higher torque. Output speed is a function of slip and supply frequency.

When the three phase input supplied to an induction motor lags the rotational position of the rotor, a torque is applied that opposes the direction of motion of rotation. This effect may be used to cause the motor to act as a generator, slowing the vehicle by converting mechanical motion to electrical current.

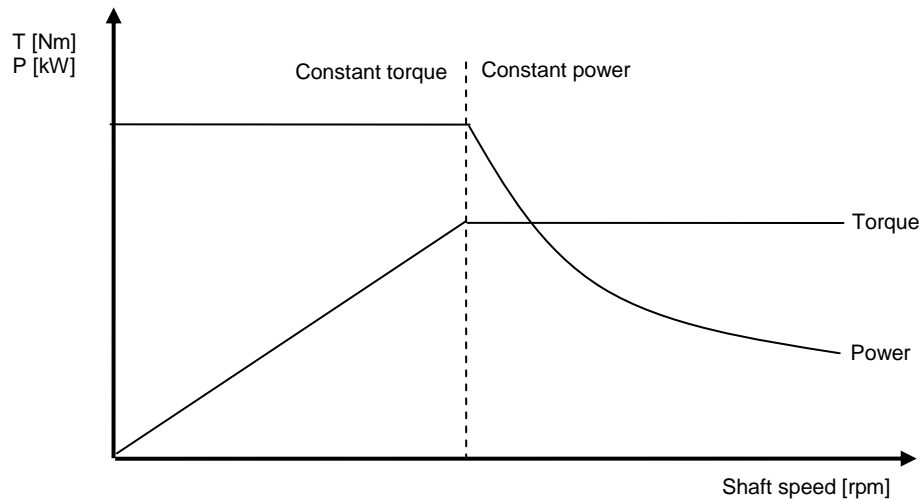


Figure 2.A - Motor torque and power vs. shaft speed

Unlike combustion engines, electric motors have their highest torque at low shaft speeds. This maximum torque is constant with respect to shaft speed up to some transition speed, where the maximum power is reached. Beyond this transition speed the maximum power is constant, with torque varying accordingly. Figure 2.A shows torque and power with respect to shaft speed for a typical motor. The availability of torque at low shaft speeds means that vehicles operated with an electric motor do not normally require more than a single gear during operation.

Induction motors have the advantage that they may be temporarily overloaded to produce higher power. The limiting aspect of overload is heat generation. A typical motor can be overloaded to provide twice the power for a period of about 30 [s] (Masrur and Mi 2006). Since peak propulsion power requirements typically occur during periods of acceleration, they are short lived. This means that the motor may be downsized, and then overloaded to meet brief peak demands.

Induction motors may have energy efficiencies of up to 96%, and work at close to maximum efficiency throughout most of their operating range (Cassio and Pontes n.d.). Less than maximum efficiency typically happens at very low torque and/or very low shaft speed.

Detailed mathematical relations exist to fully describe the state of an induction motor. These relationships are necessary in the detailed design and assessment of an induction motor, but would be cumbersome and impractical for simulating prolonged use, as in evaluating powertrain performance through a drive cycle. A number of alternate approaches can be taken. Motor simulation can be done using a simulation package such as the Powertrain Systems Analysis Toolkit (PSAT) by Argonne National Laboratory (Argonne National Laboratory 2010), or Simulink for MatLab (MathWorks 2010). PSAT and Simulink simulate motors with a condensed set of equations and relationships. For Simulink, this condensed model consists of a fourth order state-space model to represent the electrical aspect of the motor, and a second order system for the mechanical aspect (The MathWorks, Inc. 2009).

The primary goal of simulating a motor within a powertrain is to understand where energy is lost. Motors and generators have energy efficiencies that vary most strongly with shaft speed and with torque demand (Odvarka, et al. 2009), (Lukic and Emado n.d.). This fact makes it possible to estimate the efficiency of the motor using a simple lookup table, based only on shaft speed and torque. The lookup table approach is adopted by ADVISOR, a vehicle simulation toolkit developed within MatLab Simulink (AVL 2010). Lookup tables are the simplest and most computationally expedient method of simulating the operation of an induction motor.

2.2.3 Inverters

The induction motor described in section 2.2.2 - Electric Motors operates with a supply of three phase alternating current (AC), yet all portable sources of electrical energy supply direct current (DC). The prevalent method of converting DC to three phase AC is with a switched three phase inverter (Emadi 2005). A linear inverter varies output voltage between 0 and input voltage by adding an adjustable resistor in series with the output. This method entails a large energy waste as current must pass through the added resistor. A switched inverter uses a set of switches to rapidly flicker the input voltage on and off, similar to dimming a light by rapidly switching it on and off. Switched inversion does not involve an extra resistance in series with the load, and so energy losses are much lower than linear inversion.

A switched three phase inverter uses a set of six switches to produce three sinusoidal outputs. Supply frequency can be changed by increasing or decreasing the frequency of switching. Small parasitic losses are inherent as switches shed some heat in the on-state, and each change from on to off or vice versa loses some energy within the switches' snubber circuits.

Inverters can be simulated in any of the same ways as motors; PSAT, ADVISOR and Simulink all have inverter models built in. Switched electronic circuits are very tedious to simulate because of the frequent discontinuities at every state change of every switch (Bryant, Walker and Mawby n.d.). Time average models can sometimes accelerate simulation by replacing each switch with a voltage source of value equal to the time-average voltage across it and each diode with a current source equal to the time average current through it (Perreault n.d.), but this method can still involve lengthy simulation times.

If the desired outcome is simply to understand energy losses in inverters with use, their relatively simple nature lends them well to basic empirical relations in terms of switching frequency, parasitic resistances and switch losses.

2.2.4 DC/DC Converters

It is often necessary to supply electricity at a particular voltage while storing it at another. Additionally, since batteries and capacitors both have varying voltage levels throughout their range of charge, DC-DC conversion is often appropriate (Emadi 2005).

In municipal electric transmission, voltage transformation is done electromagnetically with a transformer. This approach cannot be used directly in electric transmissions since voltage is supplied with DC, instead of AC as used in transformers. Transformation may not be done after the inverter either, since the inverter supplies three phase current of varying frequency. DC-DC conversion is instead achieved using a switched approach, whereby an inductor core is magnetized with DC current from the source in one state, and this current is applied to the load in the second state. This type of conversion has many forms, but the simplest and most commonly used in electric vehicles is the switched buck-boost converter. A buck-boost

converter can transform the voltage of a DC supply either upwards or downwards depending on the duty ratio of the switch, and also serves as an electrical isolation between the source and the load.

PSAT, ADVISOR and Simulink may be used to simulate the operation of a DC-DC converter. No specific models exist within Simulink, but a model of the desired topology may be implemented and simulated. DC-DC converters are difficult to simulate for extended use for the same reason as inverters; frequent state switching is computationally expensive (Lachichi and Schofield 2006), (Yalamanchili and Ferdowsi 2006). Time average models may be used in the same way as inverters, but only provide a marginal improvement in calculation time. Like inverters, simple equations can be used to determine energy losses based on current through switches, switching frequency, and parasitic resistive losses.

2.3 EV Storage Technologies

This section covers the most relevant means available for storing and supplying electric energy for use in a vehicle. Batteries and capacitors are given special focus. The section concludes with a comparison of storage techniques, and a case for hybrid energy storage.

2.3.1 Batteries

Perhaps the oldest and most recognized method of storing electrical energy is the battery. Though other technologies have emerged, batteries, especially secondary or rechargeable cells, are still one of the best options available because of their energy density.

Many battery types are available with varying chemistries for each major category; the most common varieties are lead acid (Pb), nickel cadmium (NiCad), nickel metal hydride (Nimh) and lithium ion (Li+) (Buchmann 2003). The basic mode of operation is the same in each case, an anode and a cathode are separated by an electrolyte, which may be a liquid as in Pb or NiCad, or a gel as in Nimh or Li+. When discharging, positive ions migrate from the anode through the electrolyte to the cathode, and the reverse for charging. Figure 2.B shows a basic schematic for a Li+ battery.

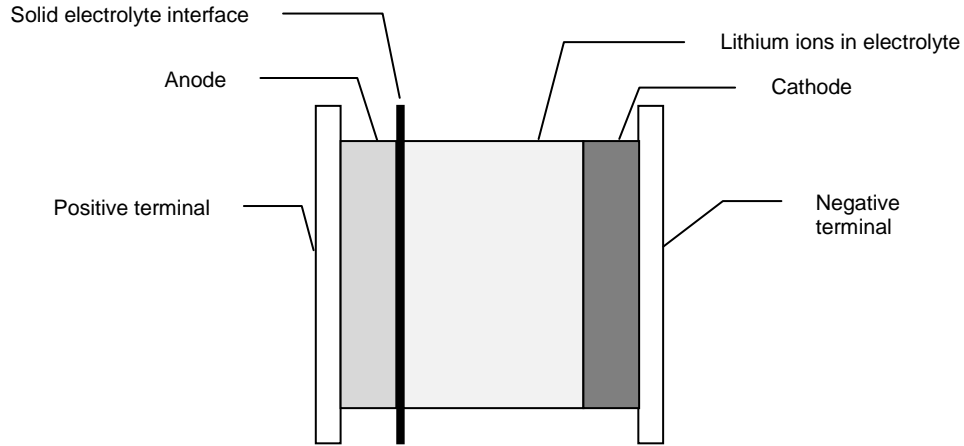


Figure 2.B - Li-ion battery schematic

Battery capacity (C) is measured in amp-hours (Ah), and the total amount of energy stored in the battery is roughly equal to the capacity multiplied by the average voltage during discharge:

$$E_{batt} = V_{avg}C \quad (2-vii)$$

A battery's state of charge (SoC) is a measure of the energy available from the battery. Batteries are typically designed to operate within a specific window of SoC, known as the SoC swing. The SoC with the lowest remaining energy in the battery is known as the depth of discharge, or DoD.

Maximum current output from a battery scales linearly with capacity, and is therefore measured in terms of capacity, using a parameter called [C]. A discharge rate of 1 [C] indicates the battery will be depleted in one hour, while a rate of 2 [C] will drain the battery in half of an hour. Current is limited by the rates for chemical reactions within the cell and by the generation of heat. It is common for batteries to have a maximum continuous rate of discharge, with a larger peak output that may be sustained for a brief period. Kokam Co. Ltd. supplies several types of Li^+ batteries with a peak output of twice their continuous rate, and can sustain this output for approximately 10 [s] (Kokam Co. Ltd. 2010).

Batteries have an internal resistance which accounts for some energy loss from the cell while charging or discharging. Partly due to internal resistance, batteries have smaller apparent capacities when discharging at high rates. This is known as the Peukert effect (Buchmann 2003).

Battery packs consist of multiple cells arranged in series and/or parallel. A set of batteries connected in series is called a string, the length of which is the stack height. The product of the stack height and number of strings gives the total number of cells in a battery pack. For instance, a battery pack with two sets of three batteries connected in series has 2 strings, a stack height of 3 and six batteries in total.

Batteries have limited service life, the length of which depends on cell chemistry, DoD, SoC swing and temperature, among other factors. With time and use, battery capacity attenuates and internal resistance grows. For most batteries, this process is accelerated with higher temperatures during storage and use, deeper discharge cycles, and high drain rates. Ideal usage conditions for a battery are moderate temperature, SoC swing and DoD, low and stable current demand with few current reversals, or microcycles. These conditions will extend the service life of the battery and yield better energy capacity per charge.

Each cell chemistry has unique characteristics that make it suitable or not for a given application. Pb batteries are simple, cheap and robust. The electrolyte, water, is readily available and so the battery can be conveniently 'topped up' if necessary. This makes them a favourite choice for use in the electrical systems of combustion engines. Additionally, Pb batteries can be serviced by careful charging and addition of electrolyte to restore some of their original capacity. Pb batteries are not ideal for electric vehicle applications because they are large, heavy, and do not tolerate deep discharge well. While recyclable, they are not considered environmentally ideal because of their lead content.

Like Pb, NiCad batteries are partially serviceable because their electrolyte, potassium hydroxide, is liquid. NiCad batteries are more tolerant to deep discharging than Pb and offer greater energy density and power density. When a current reversal occurs frequently at a similar level of discharge, a 'memory' effect occurs that reduces the cell voltage at this level of discharge, and deep discharging is necessary to reverse the

effect. Cadmium is an environmentally adverse material to extract, process and dispose of, and thus NiCad batteries are not regarded as environmentally benign.

Nimh batteries have increased energy and power density compared to NiCad's. The electrolyte is a gel, which removes the possibility of servicing the battery to restore capacity. There is no memory effect, the cells respond well to deep discharging and have good cycle life. The contents of Nimh cells are less adverse than NiCad, and may be recycled into new batteries.

Li+ batteries come in many varieties and chemistries. Li+ cells may have a rigid cylindrical case, or may be contained in a rectangular pouch, known as a lithium ion polymer battery. Li+ cells are very tolerant of reverse currents, deep discharge and high drain rate. Compared to other cells, Li+ batteries maintain their voltage throughout the discharge cycle very well. Owing to a relatively high cell voltage of 3.7 [V], Li+ batteries have the highest energy and power density of any safe chemistry operating at room-temperature, and are therefore a foremost consideration for modern EV's. Li+ batteries do have the disadvantage of poor performance at low temperatures (< about -20 [°C]) because their internal resistance increases. Table 2.2 compares several battery types (Masrur and Mi 2006), (Vetter, et al. 2005).

Table 2.2 - Battery cell comparison (Masrur and Mi 2006)

Battery Type	Specific Energy [Wh/kg]	Peak Power [W/kg]	Energy Efficiency [%]	Cycle Life	Self discharge [% per 48hr]	Cost [US\$/kWhr]
Acidic aqueous solution						
Lead/acid	35-50	150-400	>80	500-1000	0.6	120-150
Alkaline aqueous solution						
Nickel/cadmium	50-60	80-150	75	800	1	250-350
Nickel/iron	50-60	80-150	75	1500-2000	3	200-400
Nickel/zinc	55-75	170-260	65	300	1.6	100-300
Nickel/metal Hydride	70-95	200-300	70	750-1200+	6	200-350
Aluminum/air	200-300	160	<50	?	?	?
Iron/air	80-120	90	60	500+	?	50
Zinc/air	100-220	30-80	60	600+	?	90-120
Flow						
Zinc/bromine	70-85	90-110	65-70	500-2000	?	200-250
Vanadium redox	20-30	110	75-85	-	-	400-450
Molten salt						
Sodium/sulfur	150-240	230	80	800+	0*	250-450
Sodium/nickel chloride	90-120	130-160	80	1200+	0*	230-345
Lithium/iron sulfide (FeS)	100-130	150-250	80	1000+	?	110
Organic/Lithium						
Lithium-ion	118-196	400-2600	>95	1000+	0.7	700

Modelling batteries accurately is challenging, and a number of approaches exist (Chan and Sutanto n.d.), (Baisden and Emadi 2004). Most methods are mathematical models that account for the SoC, terminal voltages and demand current to predict battery response. ADVISOR, PSAT, and Simulink all employ some mathematical model to represent battery behaviour. Gravimetric specific capacity and peak power of the cell chemistries shown in Table 2.3 are arranged as a Ragone plot in Figure 2.C.

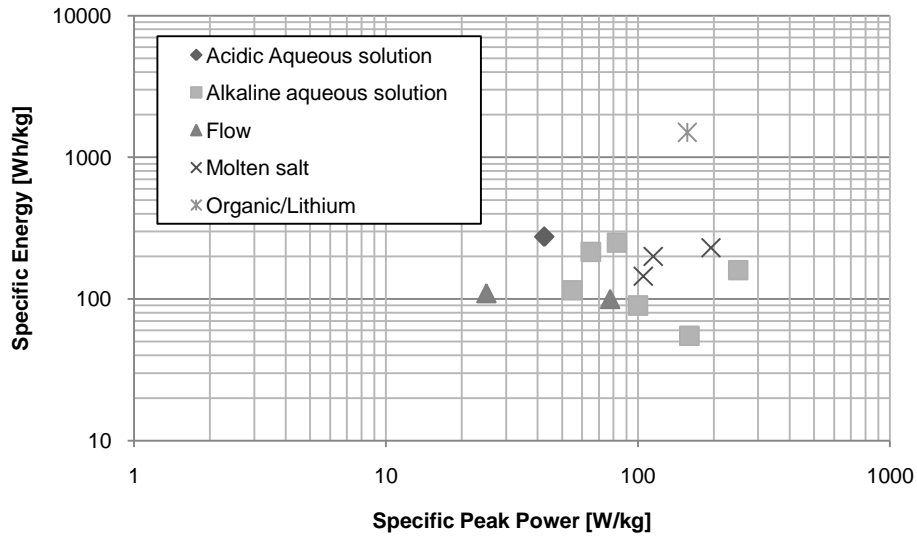


Figure 2.C - Cell chemistry specific energy vs. specific power, gravimetric

2.3.2 Ultra capacitors

Any two conducting materials separated by a dielectric gap have a capacitance, given by

$$C = \epsilon_r \frac{A}{4\pi d} \quad (2-viii)$$

where C is the capacitance in Farads, ϵ_r is the relative static permittivity, A is the overlapping area of the conductors and d is the gap between them (Conway 1999). The amount of energy stored in the capacitors is proportional to the square of the voltage:

$$E = \frac{1}{2} CV^2 \quad (2-ix)$$

Capacitors employ a dielectric layer between their plates to increase capacitance; this dielectric layer has an electric field strength limit beyond which it will fail. The dielectric limit results in a maximum voltage to which the capacitor may be charged.

Not limited by chemical reactions or movement of ions, capacitors have extremely high power delivery. However, they are very large and do not store much energy. An ultracapacitor stores more energy than a conventional capacitor by using a substrate with two porous layers separated by an extremely thin layer of insulation. By equation 2-viii, this very close separation substantially increases capacitance, and in turn stored energy. The thin separation layer means that breakdown voltage is much reduced, and so the maximum voltage across the plates is much less than conventional capacitors. Figure 2.D illustrates a conventional capacitor and an ultracapacitor. Only ultracapacitors are considered for use in this work, and so for brevity, the term 'capacitor' refers to ultracapacitors.

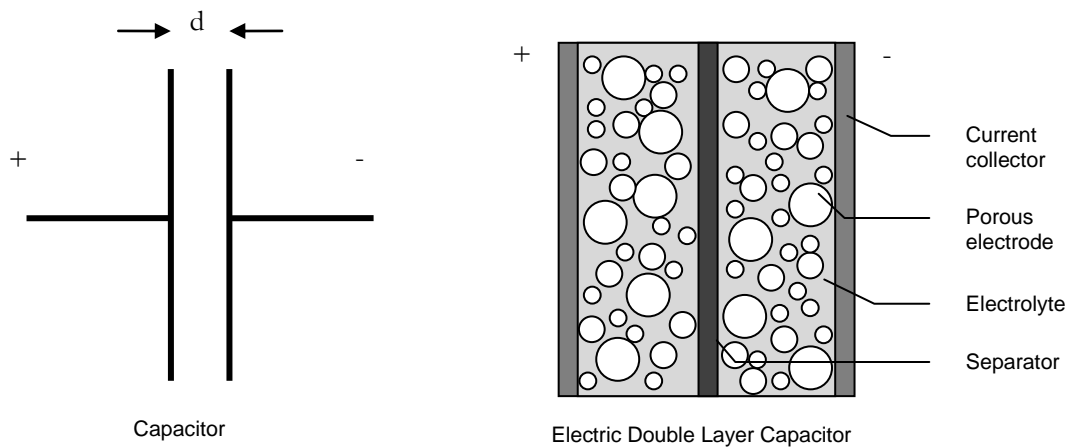


Figure 2.D - Capacitor and ultracapacitor schematic

Power output from capacitors is bounded by thermal considerations. A small equivalent series resistance (ESR) of the device results in heat generation that rises sharply with output current.

Ultracapacitors have several advantages for use in electric vehicles; they are very robust and tolerant of both mechanical vibration and cold temperatures. Ultracapacitors may be charged and discharged more than 500,000 times, and last longer than 10 years (NESSCAP Co., Ltd. 2008). While capable of very high

power delivery, ultracapacitors have very low energy density. This makes them suitable only for vehicles with very short range.

Capacitors are very simple to model mathematically, with models available in ADVISOR, PSAT and Simulink (Baisden and Emadi 2004), (Conway 1999), (Hoelscher, et al. 2006), (Jinrui and Qinglian n.d.). Simple equations in terms of current, voltage and capacitance are sufficient to understand capacitive energy storage.

2.3.3 Comparison of Storage Technologies

In this section, a wide range of energy storage methods are discussed and compared. Special attention is given to batteries and capacitors in the context of an electrically powered vehicle. Table 2.3 gives a broad overview of many different methods of energy storage (Masrur and Mi 2006), (Hilton 2010).

Table 2.3 - Comparison of storage and conversion technologies

Battery Type	Gravimetric Specific Energy [Wh/kg]	Volumetric Specific Energy [Wh/m ³]	Energy Efficiency [%]	Cycle Life	Self Discharge [%]
Hydrocarbon					
Gasoline	12,890	9.5×10^6	<30	-	0*
Hydrogen	39,720	Liquid: 2.8×10^6 700 bar: 1.6×10^6	Combustion: <25 Fuel cell: 50	-	0**
Natural Gas (250 bar)	14,890	10.1×10^4	?	-	0*
Kinetic					
Flywheel	12-30	?	80	-	100***
Electrostatic					
Ultracapacitors	3-5.5	6.8×10^3	>95	500,000	1
Electrochemical					
Lead/acid	35-50	1×10^5	>80	500-1000	0.6
Nickel/cadmium	50-60	3×10^5	75	800	1
Nickel/metal Hydride	70-95	1.4×10^5	70	750-1200+	6
Lithium-ion	118-196	$2-4 \times 10^5$	>95	1000+	0.7

*Leakage and/or vaporization is possible

**Diffusion through pressure vessel walls is common

***Flywheel spin-down time is approximately 30 minutes

Portable energy storage and conversion for use in electric vehicle propulsion is ideally energy and power dense, usable indefinitely, cheap and convenient to build and refuel or recharge, is energy efficient,

robust, and poses no safety or environmental hazard. No method presently known achieves all of these objectives perfectly.

Gasoline and other hydrocarbons are among the most energy dense storage solutions, even though the poor efficiency of combustion greatly reduces the amount of useful energy available from these sources. Hydrocarbons are still the best option available for extended driving range. A gas tank is made inexpensively, may be filled in minutes, used for a lifetime, and tolerant of adverse temperatures and mechanical vibration. Power is limited only by the maximum rate of pumping gasoline to the engine. Hydrocarbons, especially gasoline, are mostly manufactured fuels with extensive environmental and safety hazards associated with their production and use. Gasoline, manufactured from crude oil, is expected to become scarce in the far term (Styles 2010).

Hydrogen is an alternative hydrocarbon that may be used to generate electricity as in a fuel cell, but may also be used in combustion. The efficiency of combustion is much less than that of electrical generation, and has otherwise very similar characteristics to gasoline combustion. While the gravimetric energy density of hydrogen is much higher than gasoline, it is somewhat impractical to store. Compressed hydrogen tanks are much larger and heavier than gas tanks, and if liquefied hydrogen is used, diffusion through the vessel wall is significant (Masrur and Mi 2006). In either case, the storage vessel may be refuelled quickly and conveniently if appropriate facilities are available, but needs consideration of the risks of explosion. The power delivery of hydrogen is limited in fuel cells by the size of the fuel cell stack; a stack large enough to meet peak vehicle demands is large, heavy and costly. Fuel cells are very sensitive to temperature and mechanical vibration.

A flywheel is perhaps the most direct storage of energy, since no energy conversion takes place between flywheel and transmission, storage and conversion are accordingly efficient. Very low energy density, lack of any convenient way to recharge, and rapid rate of loss makes mechanical storage suitable only for capturing regenerative braking energy.

Batteries and ultracapacitors are highly energy efficient, may be recharged with electricity generated from any source, and are highly energy efficient. Safety considerations are present but less serious than those

of hydrocarbons. Batteries and ultracapacitors both suffer from limited power output and energy density. While ultracapacitors can easily achieve the desired power output, they do not store enough energy for propulsion of more than a few kilometres. Batteries suffer from a less severe deficit of both power density and energy density. Both technologies make a compromise between power and energy. Figure 2.E shows a Ragone plot of volumetric energy and power density for batteries and capacitors. On this power-energy spectrum, capacitors lie at the far end of the power side and batteries cover a range of the energy side.

Presently no single electrical storage device exists between batteries and capacitors on the power-energy spectrum. Among the range of batteries available, most electrified vehicles use those that are power optimized in order to meet peak vehicle demands, sacrificing extra capacity that would have been available from energy optimized batteries.

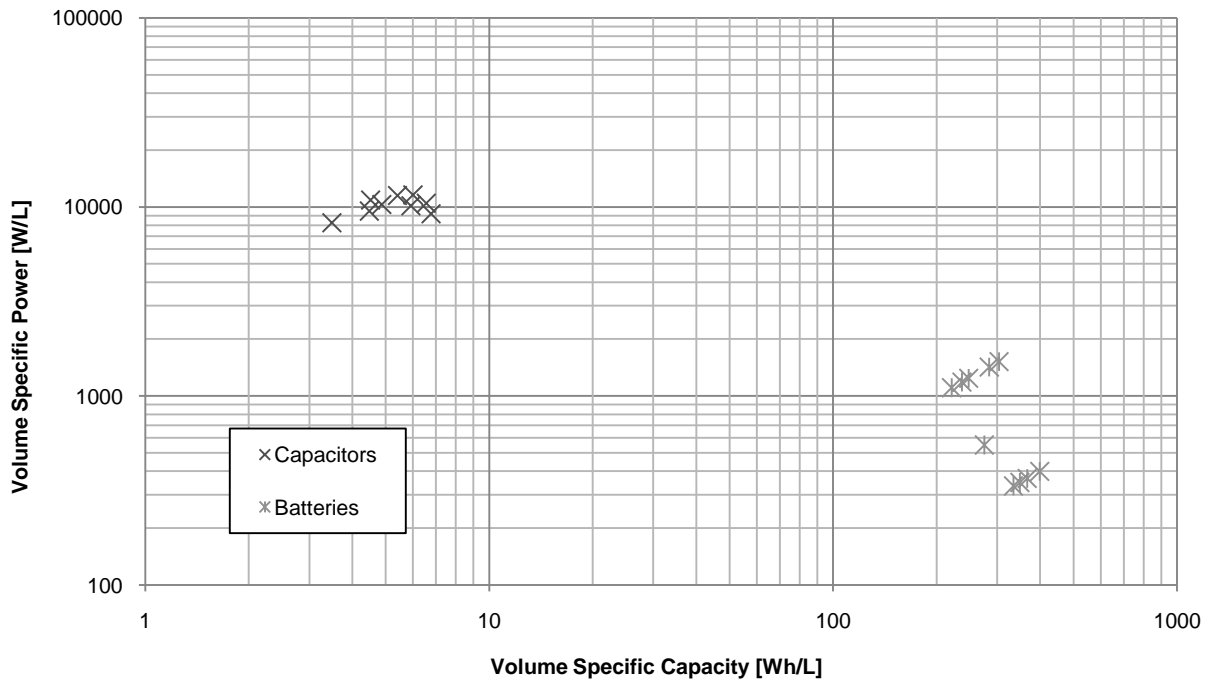


Figure 2.E - Energy density vs. power density, volumetric

2.3.4 Hybrid Energy Storage

In section 2.3.3 it was shown that every storage technology, especially electric storage devices, have a unique set of advantages and disadvantages. It can be advantageous to combine more than one electric storage device, in order to realize the benefits of each. Specifically, a power optimized device can be paired with an energy optimized device, such that energy capacity is increased while power delivery is sufficient to meet peak demands. The concept is similar to using an accumulator in a hydraulic circuit to shave peak demands from the pump. To reduce the size of its fuel cell, the Honda FCX Clarity employs a bank of ultracapacitors to handle peak demand, while continuous running demands are supplied by the fuel cell stack (Honda Motor Co., Ltd. 2010).

Hybrid storage systems using batteries and capacitors are among the most commonly studied, and it has been shown that these can be more versatile, increase component service lives and efficiency while reducing cost and mass relative to storage systems using only batteries or only ultracapacitors (Hoelscher, et al. 2006).

By adding a bank of ultracapacitors to a pack of batteries, the battery pack may be selected for energy density, rather than power delivery, and so energy capacity increases. Since capacitors are well suited to frequent current reversals, they may be used to absorb regenerative braking energy. This effect combined with peak shaving mean that the battery load becomes more stable and reverse currents can be eliminated, which is expected to result in longer battery service life and increased effective capacity.

Since the energy and power devices will have different voltage levels, DC-DC conversion requirements change (Lachichi and Schofield 2006), (Lukic, et al. 2006), (Yalamanchili and Ferdowsi 2006), (Hoelscher, et al. 2006). Specifically, each device must each have a unique link to the vehicle power bus. Simply connecting batteries and capacitors together in parallel would result in the battery supplying most of the load, since capacitor voltage is linear with SoC. Each device may have its own DC-DC converter, with the converters connected either in parallel or in series. Alternatively, a single, dual-input DC-DC converter may

be used to draw from sources simultaneously. Figure 2.F shows four methods of coupling batteries and ultracapacitors.

It is shown by Lukic, et al (Lukic, et al. 2006) that the ideal way to couple two sources of different voltage is a dual-input DC-DC converter, of which various topologies exist.

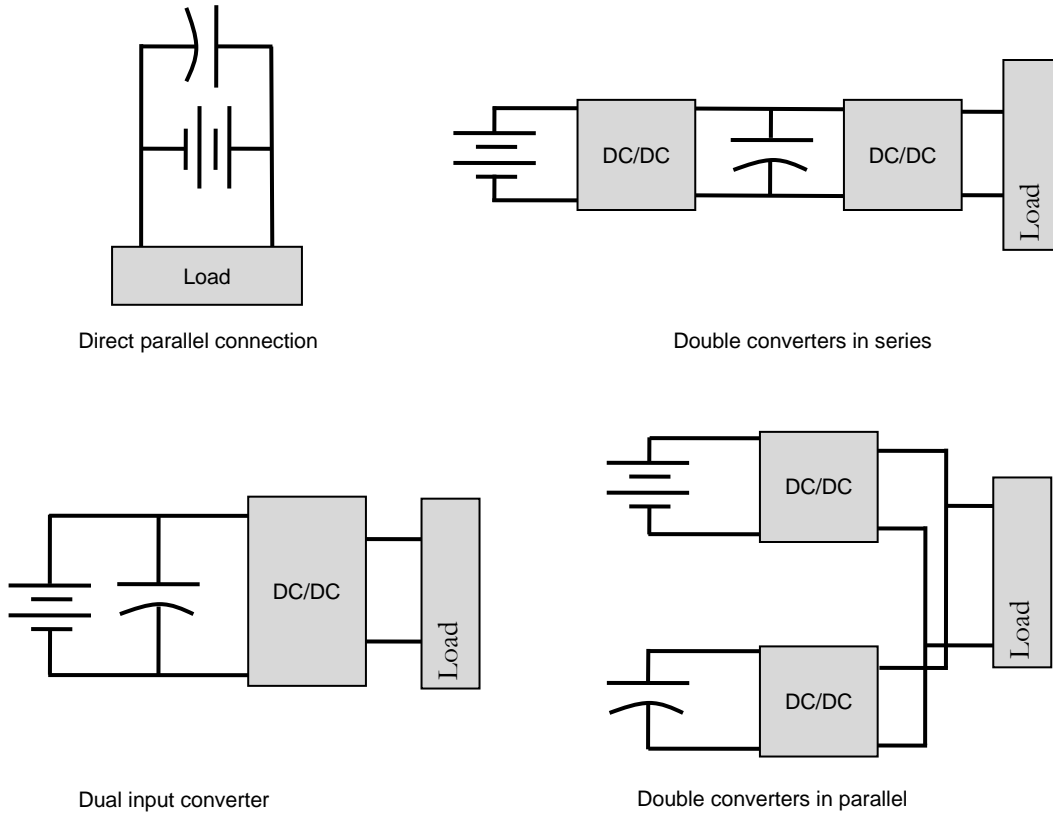


Figure 2.F - Battery-capacitor coupling options

2.3.5 Hybrid Control and Power Management

A unique requirement of an energy storage system using multiple sources is the need for a control scheme to allocate demand across the sources. Power requirements vary widely throughout a drive schedule, with peak demands during acceleration of more than three times the average power output of the whole drive cycle (Rossario, et al. 2006). A hybrid energy storage system meets average propulsion demands with a high

capacity energy system, and peak vehicle demands with a high power system. A control scheme, or energy management system (EMS) should then allocate average running demand to the energy system and peak demands to the power system.

There are many strategies for the design of an EMS. Most approaches consider inputs such as the demand current, SoC of the battery, maximum output of the battery, vehicle speed and acceleration, etc. A simple rule based system will use these inputs to allocate power with logic statements such as (Jalil, Kheir and Salman 1997)

"If demand current > maximum battery current, then battery power = battery maximum and capacitor power = demand - battery maximum"

A rule based system is simple and easy to implement, but can result in discontinuities when inputs cross boundary values. Fuzzy logic control offers a similar, but more stable approach (Kisacikoglu, Uzunoglu and Alam 2006). A fuzzy based system sorts input values into overlapping categories with membership functions. By example, vehicle speed may lie on a range of slow to fast, but a value in between slow and fast may have a membership value of 30% fast, 70% slow. A fuzzy rule base evaluates logical statements based on the inputs in a similar fashion to a simple rule base. Output of the rule base lies on a similar sliding scale to the inputs, returning one or more results. When multiple results are returned, an amalgamation is made to deliver the final result. The method can be thought of as a way to generate a smoothly transitioned piece-wise output function of the input parameters. The output function is tolerant of error or rapid change of inputs. Fuzzy logic controllers are very well suited to EMS, but require much trial and error to implement well.

2.4 Powertrain Evaluation

Designing and developing a vehicle powertrain or part thereof, whether propulsion is electric or combustive, presents a sizeable gamut of problems and considerations. As with any design discipline, the process is iterative and very reliant on the ability to test and evaluate designs to address problems and make incremental improvements.

Prototyping and physical testing is the most positive way to assess a design, but is also the most costly and time consuming. Given the many revisions often necessary to develop a powertrain or a component of it, prototyping and physical testing is typically restricted to design milestones very late in the design process.

Computer modelling and simulation is a much faster, more flexible and less expensive approach to understanding a propulsion system. Experienced designers can create models in a matter of days, changes can be made easily, and simulation can be performed rapidly and autonomously. Models can be made with a degree of complexity to suit the purpose. For instance a highly detailed model of an engine can be simulated to comprehensively understand its operation, or it can be represented with a very simple model if its behaviour within a wider system is desired. The speed, cost, ease and accuracy of simulation account for its major adoption in the practice of powertrain and propulsion development.

The intersection of prototyping/testing and modelling/simulation is known as hardware in the loop (HIL) (Winkler and Guhmann n.d.). HIL uses a combination of computer models and physical hardware to perform tests. For instance, a HIL test in the development of a hybrid power train may include a physical engine and computer models of the electric motor, energy storage and power electronics. The engine would have computerized inputs and be attached to a dynamometer to feed back information to the simulation. This arrangement could be used to assess the interaction of the engine and motor to propel a vehicle in order to optimize the controller allocating torque between the two. Like prototyping, HIL testing is highly expensive and time consuming to perform.

Fortunately, many options are available for modelling and simulation. PSAT, ADVISOR and Simulink are all popular choices. ADVISOR, a program based on the Simulink platform, offers a number of common devices and powertrain configurations modelled using operating efficiency tables. The lack of any physics based simulation means ADVISOR is very rapid, and the accuracy of the results is sufficient in most cases (Hoffman, Steinbuch and Druten 2006).

The platform for ADVISOR, Simulink, contains a library of electromechanical devices and power electronics that can be used to model a powertrain (Lin, et al. 2001). The devices are modelled from physical processes, which means simulation can take a long time, particularly for switched power electronics which have frequent state changes requiring iteration. Power electronics specific applications are available to simulate switched systems much faster, some of which can interface with Simulink (POWERSIM n.d.).

When simulating a powertrain in ADVISOR, a backwards-facing approach is taken. This means the vehicle speed follows the input drive cycle exactly, and it is assumed a-priori that the vehicle is able to follow the drive cycle. Check values must be examined post-simulation to confirm that traction, torque, and other vehicle limits were not violated in the simulation. Energy usage and other measurements are made of the powertrain in the course of keeping pace with the drive cycle.

Absent from the backwards-facing approach is any consideration of the throttle or brake pedals. PSAT, developed by Argonne National Laboratory, takes a forward-facing approach, whereby a driver module attempts to follow the drive cycle as closely as possible using a simulated throttle and brake. In a forward-facing simulation, the test vehicle will not follow the input drive cycle unless the powertrain is capable of doing so. Forward facing simulation is regarded as more accurate than backward facing, though simulation times are longer (Xiaomin, et al. 2009). Backward or forward facing simulation is possible in Simulink, depending on how the model is designed.

In this chapter, several technologies for storing energy in vehicles were described. Similar discussion was given to converting energy in electric vehicles. The chapter concluded with a comparison of different means of evaluating a given powertrain for performance and energy efficiency. The intention of this study is to determine whether hybrid energy storage is a viable approach to balancing the energy capacity of the storage system with its power delivery, and if such a storage system might extend have an extended service life compared to a battery only system.

3.0 Vehicle Configuration and Simulation

In this section, the design strategy for the hybrid energy storage systems is presented. The complete approach to modelling and simulating the modified Pacifica is explained, as well the topology and components of the drive train are specified. To begin with, the propulsion requirements of the Pacifica are estimated.

3.1 Vehicle Configuration

To fully examine all of the potential advances that are possible with electrification, it is pertinent that the Pacifica be capable of all-electric operation, up to and including highway travel. Ideally, the vehicle will have as much all-electric range as possible. For simplification, this study will not consider use of the combustion engine. The vehicle is treated as having strictly electric propulsion, and so the electric propulsion system must be capable of meeting the full running requirements as estimated by equation 2-i. Power requirements are twofold; the powertrain and energy storage system must be able to; (1) continuously supply enough power to operate the vehicle at highway speeds, taken here as 120 [km/h], and (2) sustain power peaks encountered under acceleration to highway speed.

Requirement (1) is determined by the sum of rolling resistance and aerodynamic drag at highway speed. Requirement (2) is estimated simply as the constant power required to accelerate from 0 to 97 [km/h] (60 [mph]) in a period of 10 [s]. For reference, the stock vehicle's 0-60 [mph] time is approximately 9.3 [s].

The coefficient of rolling resistance is estimated at $C_r = 0.01$ (Masrur and Mi 2006) and the vehicle curb weight of 2121 [kg] (Allpar 2010), is expected to increase to approximately 2500 [kg] after modification. Exact vehicle weight depends on the storage system used. The Pacifica has an aerodynamic drag coefficient of $C_d = 0.35$ and frontal area $A = 2.82$ [m²] (New-cars.com 2004). In accordance with equations 2-i through 2-vi, the continuous power requirement for travel at highway speed is 30 [kW], and the peak power is 90 [kW], or 41 [hp] and 121 [hp] respectively.

Neglecting losses, the powertrain and energy storage system of the Pacifica must be able to supply at least 30 [kW] continuously and up to 90 [kW] for periods of up to 10 [s]. Of equal design importance to

power is the amount of current required to supply the power. Determining operating current requires selection of a bus voltage with which to supply the inverter and motor, as well as a nominal supply voltage with which to store energy.

For reference, the General Motors EV1 had a supply voltage and bus voltage of 312 [V] (General Motors 2001). Using equal supply and bus voltages reduces DC-DC conversion requirements, and higher voltages generally translate to lower operating current and resistive losses. For the purposes of this study, the modified Pacifica will use a supply and bus voltage of 320 [V]. Given that current is proportional to power and the inverse of voltage, the current required to supply 198 [kW] at 320 [V] is 619 [A].

3.1.1 Powertrain

For this study, the drive train topology proposed by Samborsky will be adopted (Samborsky 2006). In this configuration, motor/generators (MGs) are connected to the differentials of both front and rear axles with single speed gear reductions and the internal combustion engine (ICE) drives the front axle using the existing four-speed automatic transmission. A hybrid electric energy storage system is used to power the electric propulsion system, which may use batteries and capacitors or two types of batteries. Figure 3.A shows an overview of the powertrain using batteries and ultracapacitors.

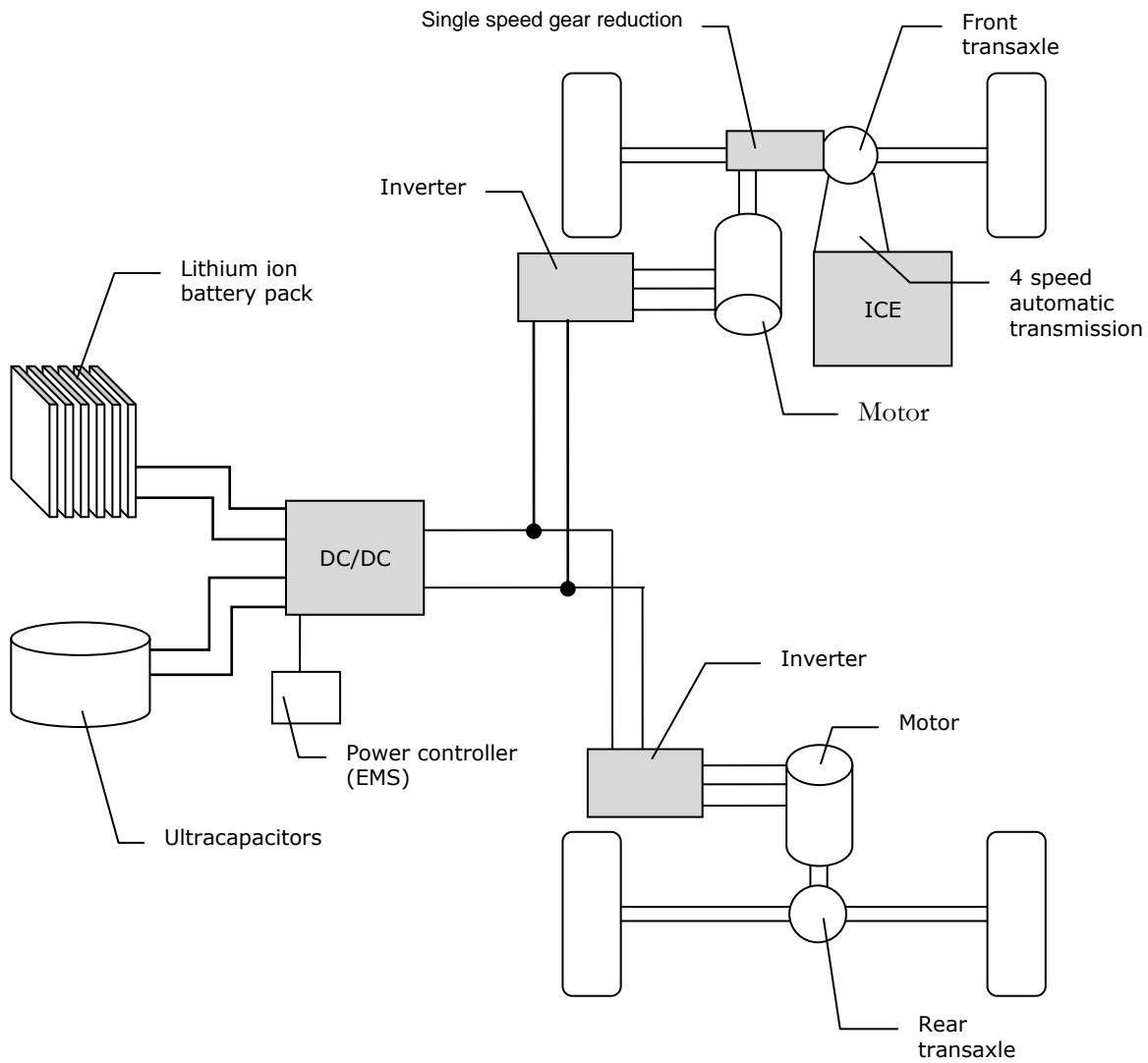


Figure 3.A - Powertrain overview

The same three-phase AC induction motor and corresponding switched inverter is to be used at each axle. Allocating electric drive at each axle allows for dynamic handling effects to be studied and for maximum energy recovery from regenerative braking. With a view to maximize efficiency, only one of the two motors will operate at a time, unless torque demand requires both to be used (Mendes 2006). Furthermore, the single speed gear reduction for each MG was selected such that the MGs would operate at the highest rotor speeds without exceeding maximum rotor speed at highway velocity. Assuming a maximum rotor speed of 5500

[rpm], the single speed gear boxes are set to give a final drive ratio of 6:1. This results in rotor speeds of 5335 [rpm] when travelling at 120 [km/h].

The DC-DC converter is a bidirectional, integrated buck-boost, buck-boost converter of similar topology to that discussed by Lachichi and Schofield (Lachichi and Schofield 2006). A design for the inductor used in the converter was prepared by the Author, and is detailed in Appendix B. The inductor uses four separate gapped cores in parallel, with a total inductance of 25 [μ H]. Design of the inductor follows the core geometry approach developed by McLyman (McLyman 2004). Power allocation is applied through the DC-DC converter by a controller programmed with the appropriate EMS. Design of the EMS is discussed in section 3.1.2, Hybrid Energy Storage Design Strategy.

3.1.2 Hybrid Energy Storage Design Strategy

A successful hybrid energy storage system (HESS) must achieve some combination of (1) increased vehicle performance by supplying more power, (2) extended storage system service life, (3) improved cold weather performance, or (4) reduced storage system volume or weight. Furthermore, a successful HESS will not unduly compromise any other aspect of the storage system.

Two options for a power device are considered here: ultra high power Li+ batteries and ultracapacitors. High capacity Li+ batteries are used as the energy system in either case. Ultra high power batteries give high power capability in a much smaller package, leaving room for extra energy batteries, but a reduced total power output. Detailed parameters of the ultracapacitors and all battery models used in this study are given in Appendix C.

Limited space is available in the vehicle for energy storage. This space must be appropriately shared among the energy and power systems. A larger energy system increases the total energy capacity and range of the system, and nominal load is spread among more energy cells, reducing energy system stress. A larger power system increases the maximum power available and the duration of peak output of the system, while reducing stress by spreading load across more power components. In section 3.1, Vehicle Configuration, it

was shown that peak output should be able to sustain acceleration of the vehicle to highway speed, requiring 90 [kW]. Exceeding this power requirement is of limited benefit; thus the power system should be only large enough to meet it, leaving the maximum amount of room available for the energy system, and by extension, vehicle range.

Design of the hybrid storage system for the Pacifica follows a strategy based on vehicle kinetic energy. The largest total amount of kinetic energy to be supplied during a given high power peak is comparable to the kinetic energy of the vehicle at its maximum expected speed, a highway velocity of 120 [km/h]. This suggests that the power system should have a useable capacity that is at least large enough to accommodate this amount of energy, plus a safety factor to accommodate for conversion efficiency. For the assumed vehicle mass of 2500 [kg] travelling at 120 [km/h], the vehicle's kinetic energy is 1.4 [MJ], or 389 [Wh].

Two power systems were designed: one using ultracapacitors and one using ultra high power batteries. Details of each are given in Table 3.1 (Kokam Co. Ltd. 2010), (NESSCAP Co., Ltd. 2008).

Table 3.1 - Power system properties

	Ultracapacitor	Ultra high power batteries
Cell properties		
Maximum voltage [V]	2.7	4.2
Minimum voltage [V]	0.5	3.5
Capacitance [F]	5000	-
Total energy capacity [Wh]	5.1	27
SoC swing (Max/Min)	100/3.33	70/40
Useable energy capacity [Wh]	4.9	8
Nominal discharge current [A]	Not specified	36
Maximum discharge current [A]	2547	144
Duration of maximum discharge [s]	1	10
Maximum power output [kW]	6.9	0.6
Internal resistance [mΩ]	< 0.33	0.3 (estimate)
Pack properties		
Stack height	120	84
Strings	1	1
Total cells	120	84
Maximum voltage [V]	324	353
Minimum voltage [V]	60	294
Capacitance [F]	42	-
Total energy capacity [Wh]	608	2240
Useable energy capacity [Wh]	587	672
Nominal discharge current [A]	Not specified	36
Maximum discharge current [A]	2547	144
Duration of maximum discharge [s]	1	10
Maximum power output [kW]	825	51
Internal resistance [mΩ]	40	25.2

Both systems are designed to have operating voltages of approximately 320 [V], and a capacity of at least 150 [%] of the vehicle's maximum kinetic energy. A safety factor of 1.5 accommodates for energy losses in the drive train. The capacitor system is designed not to discharge below 60 [V], and not to exceed its maximum potential of 324 [V]. To reduce the fatigue of severe demand fluctuation and current reversals, the battery system is designed to operate within a relatively narrow SoC swing of 40-70 [%]. This SoC restricted swing is common for batteries in gas-electric hybrid vehicles to prolong battery service life (Santini 2009).

The EMS controlling the hybrid energy storage system must also reflect the kinetic energy strategy. Observe that if the vehicle is at rest, it is next likely to accelerate and will require energy from the high power system to do so. Similarly, if the vehicle is travelling close to its maximum velocity, the most likely event is a

deceleration, requiring the power system to absorb energy from regenerative braking. This suggests that the energy stored within the power system should be related to the speed of the vehicle, being fully charged when the vehicle is at rest, and relatively drained when the vehicle is at high speed.

A kinetic energy based EMS can be implemented by creating a reference function of power system SoC to vehicle speed, and adjusting power system output to match the reference function. This causes power system output to scale positively with acceleration, becoming negative under regenerative braking. Cruising requirements during constant velocity are supplied by the energy system.

Note that only a cursive attempt is made at optimizing the parameters of the storage system. Full optimization would include a comprehensive study of the effects of different energy and power system stack heights and string numbers and bus voltage. Due to the large design space, genetic algorithms present an ideal way of determining the best makeup of the hybrid energy storage systems (Huang, Wang and Xu 2006), (Montazeri-Gh, Poursamad and Ghalichi 2006), (Wang 2005).

3.2 Simulation Structure

To assess hybrid energy storage systems, a powertrain model was developed to simulate and evaluate system performance under a variety of conditions. This section explains how the powertrain was modeled.

3.2.1 Overview

Because of its simplicity and availability, computer modelling and simulation was the chosen method of evaluating the performance of a powertrain using hybrid energy storage systems. Among the prevalent options to do so, PSAT, ADVISOR and Simulink for MatLab, Simulink is the most versatile and this made it the simulation tool of choice for this investigation.

The model of the electric powertrain for the modified Chrysler Pacifica uses a combination of efficiency tables and empirical relationships to represent its individual components. The components are organized into subsystems that connect together and operate dependently. The subsystems are, in order of

calculation: (1) drive cycle motion, (2) drag force, (3) power and acceleration requirements, (4) motor and transmission simulation, (5) inverter simulation, (6) DC-DC converter simulation, (7) energy management system calculation, and (8) hybrid energy storage system simulation. These subsystems are illustrated in Figure 3.B. The complete system, except for drive cycle input and EMS calculation, can be seen in Figure 3.C, which shows an overview of the powertrain model developed in Simulink.

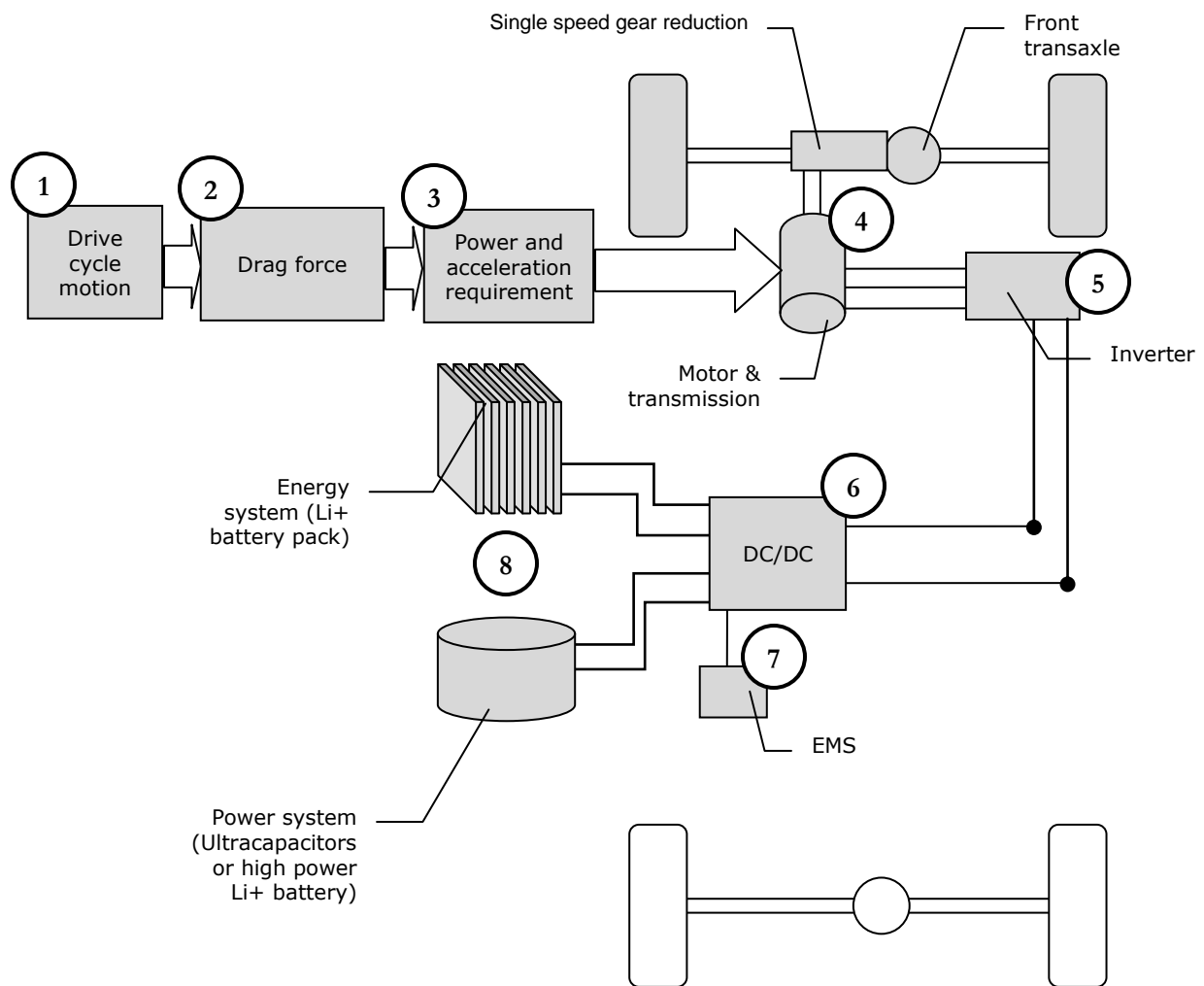


Figure 3.B - Powertrain calculation procedure

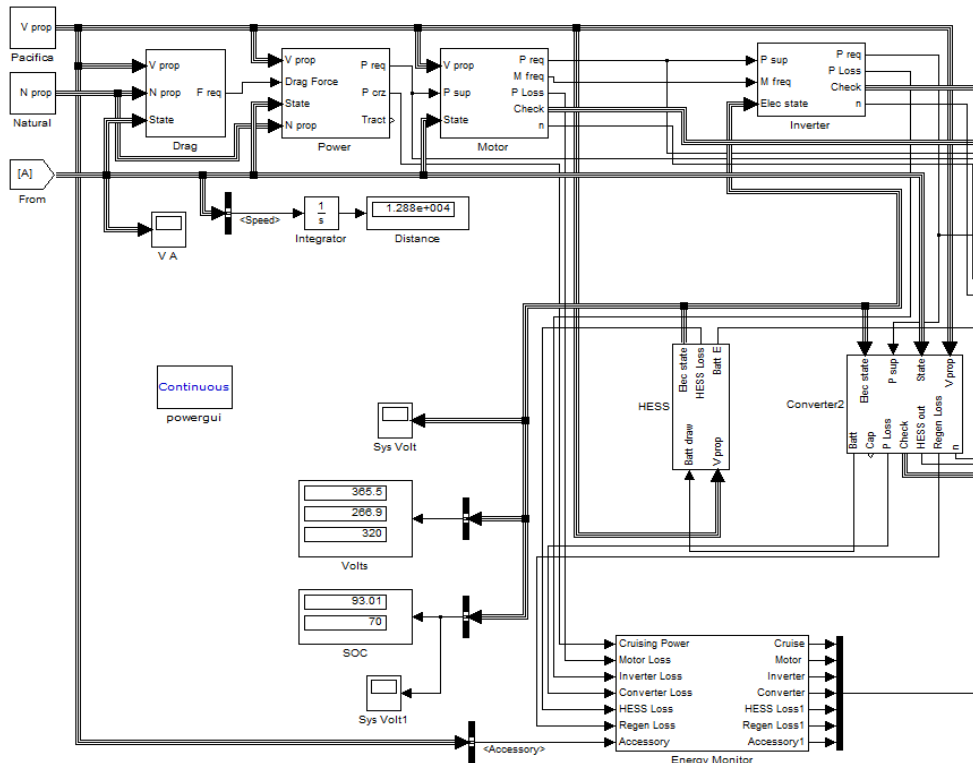


Figure 3.C - System overview

3.2.2 Inputs

The model leverages three inputs: vehicle properties, natural properties and a drive cycle. The natural properties module contains constants for the density of air and acceleration due to gravity. These constants are used as appropriate throughout the model. Similarly, a vehicle properties module contains a collection of parameters necessary to model the vehicle and its powertrain. The complete list of parameters included in the vehicle module and their units follows:

- Vehicle mass (dependent on number and mass of components of storage system) [kg]
- Coefficient of drag
- Frontal area [m²]
- Coefficient of rolling resistance
- Wheel radius [m]

- Transmission ratio
- Motor ratio
- Number of energy strings
- Energy string stack height
- Energy cell capacity [Ah]
- Energy cell mass [kg]
- Number of power strings
- Power string stack height
- Power cell capacity [Ah] for batteries or [F] for capacitors
- Power cell mass [kg]
- Vehicle weight distribution (front/rear)
- Accessory load [W]

Data for all five of the drive cycles used in this investigation are available from the United States Environmental Protection Agency website (United States Environmental Protection Agency 2008), and consist of velocity measurements at one second intervals. These velocity data, part (1) in Figure 3.B, were used to determine distance travelled and acceleration within a spreadsheet. Velocity and acceleration were then imported into separate lookup tables within Simulink. Given an input signal corresponding to simulation time, these lookup tables return the instantaneous velocity and acceleration of the vehicle respectively. A time repeater, based on the duration of the drive cycle, is used to cause the lookup tables to return a repeating signal, useful if an extended simulation of more than one cycle is required. A sample drive cycle input subsystem is shown in Figure 3.D.

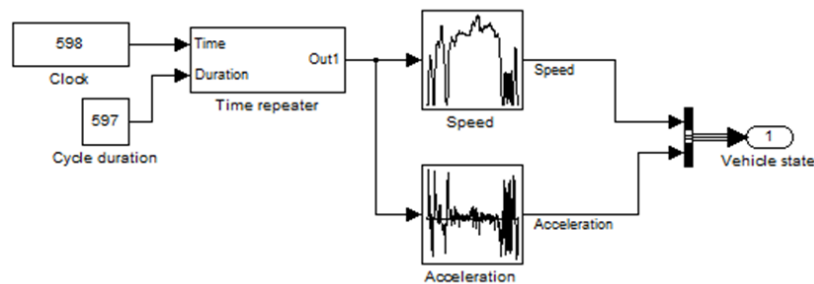


Figure 3.D - Drive cycle input

3.2.3 Vehicle Drag Force

Given vehicle speed, drag force may be determined; part (2) in Figure 3.B. Rolling resistance and aerodynamic drag are determined as per equations 2-iv and 2-v respectively. Drag force is returned as shown in Figure 3.E.

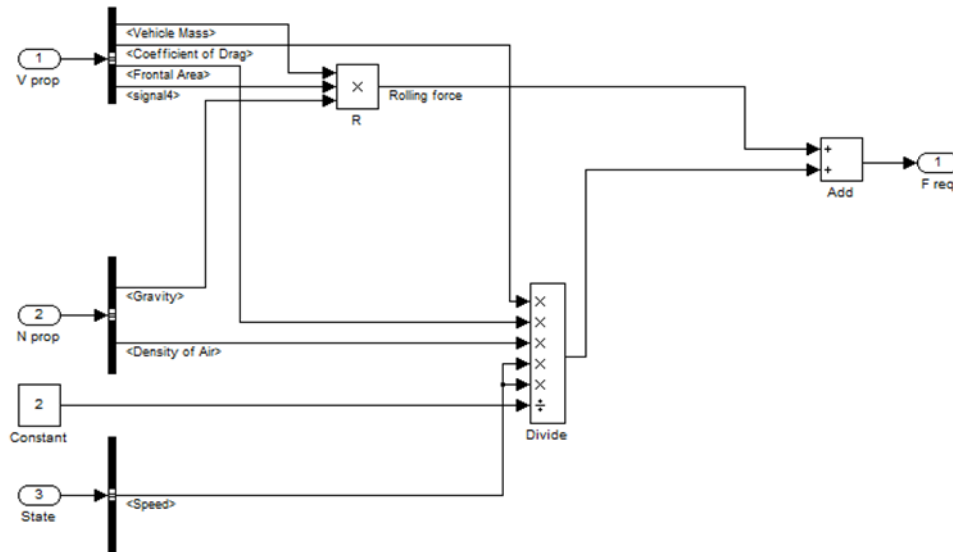


Figure 3.E - Drag force schematic

3.2.4 Running power

Given drag force and vehicle speed, cruising power may be found - part (3) in Figure 3.B. Given acceleration, the total mechanical power required is obtained. As per equations 2-i and 2-ii, total power is calculated as shown in Figure 3.F. As a consistency check, the available traction and associated maximum possible acceleration are calculated. Actual acceleration is subtracted from available traction to return the margin of traction. This value must be positive at all times to confirm that the vehicle's front wheels have not lost traction. A running minimum block returns the lowest margin of traction throughout the drive cycle.

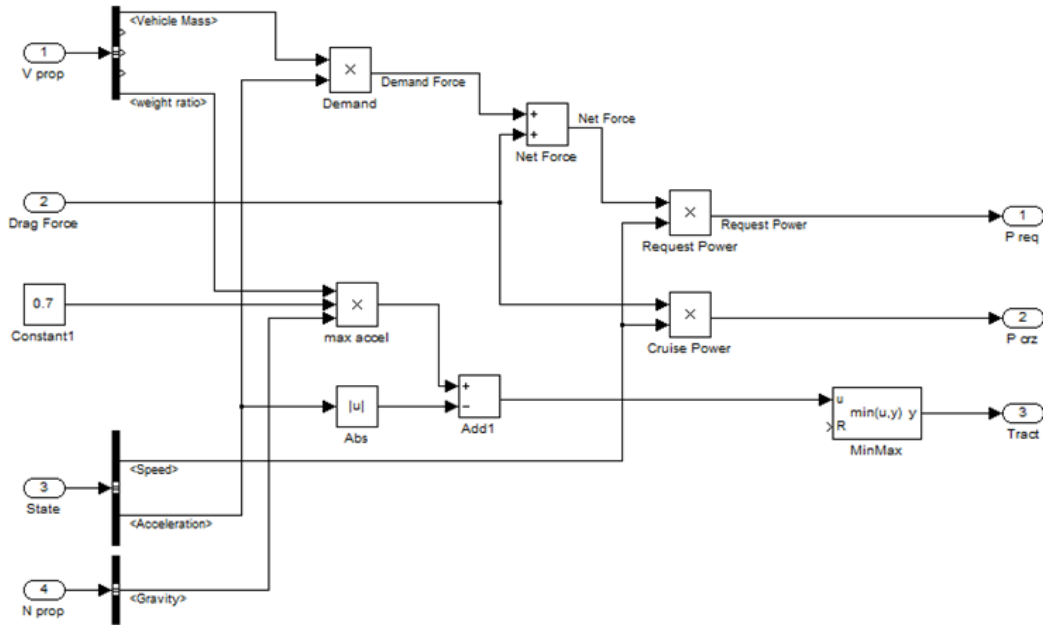


Figure 3.F - Running power schematic

3.2.5 Motor

While the Pacifica is to use separate motors at the front and rear axles, the overflow torque split method proposed by Mendes (Mendes 2006) mandates that only a single motor should be used to provide all torque requirements unless demand cannot be met by a single motor. With allowances for periodic overloading, this leads to an important simplification for this powertrain model: both motors are modelled together as a single machine. A three phase asynchronous induction motor model was modelled in Simulink, with shaft speeds determined from wheel size and transmission ratios. This is part (4) in Figure 3.B. Measurements of efficiency were made at a range of shaft speeds and demand torque. These measurements were then consolidated to produce a lookup table of motor efficiency vs. shaft speed and torque to represent the energy characteristics of the motor. Though the expected trend of low efficiency was apparent at low shaft speed and low torque, the maximum efficiency of the motor was unrealistically high, with an efficiency of near unity. To compensate for this, a gain of 0.93 was applied to the output of the efficiency table. This brings the maximum efficiency of the simulated motor into better agreement with real motors (Cassio and Pontes n.d.).

Vehicle speed, wheel radius and transmission ratio may be used to find the instantaneous speed of the rotor. Wheel radius, transmission ratio and the total mechanical power requirement determine the torque demanded of the motor. Motor torque and shaft speed are then used as inputs to the motor efficiency lookup table, which returns the fraction of energy used by the motor that is converted to mechanical power. This fraction is used to determine the input electrical power required to produce the desired mechanical output power.

The difference in speed of the motor and its input electrical frequency is known as the motor ratio. The product of motor shaft speed and motor ratio give the necessary electrical input frequency, which is output from the motor subsystem for use in the inverter subsystem.

Minimum/maximum checks are performed for motor efficiency, shaft speed and torque demand. These are used to identify invalid simulation output. Figure 3.G shows the motor subsystem.

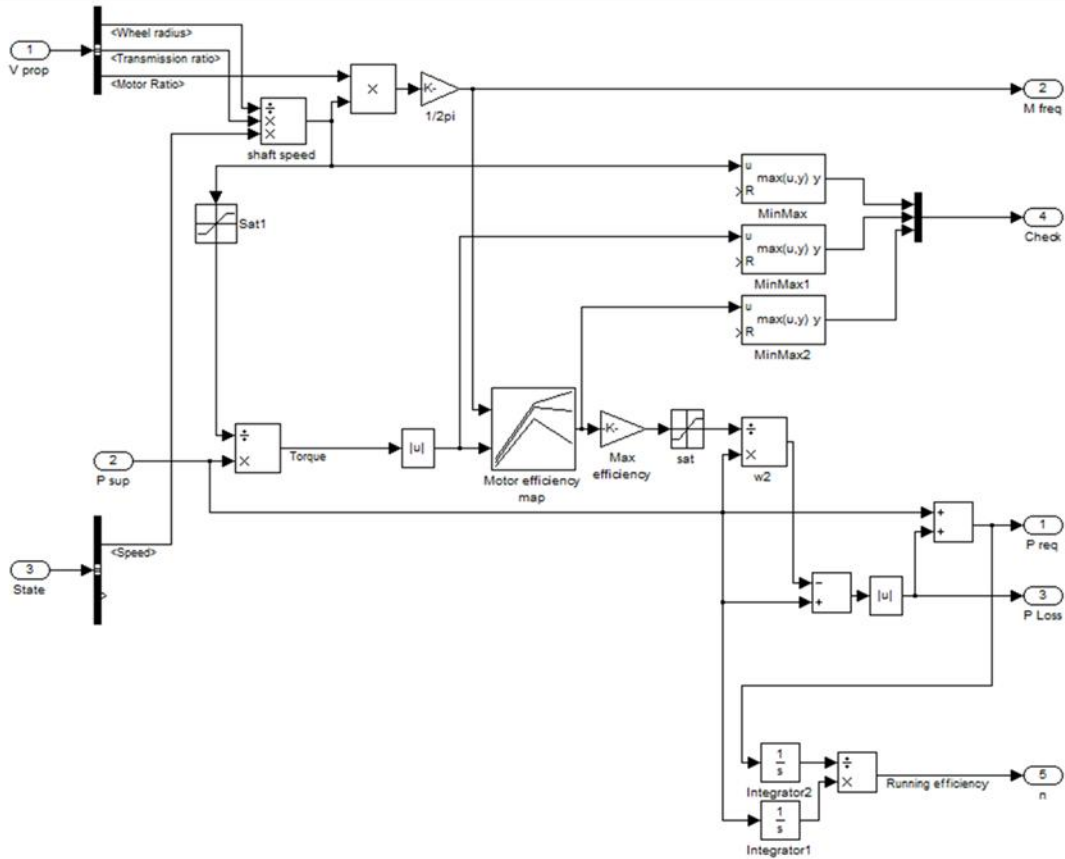


Figure 3.G - Motor schematic

3.2.6 Inverter

The inverter module uses empirical relations to estimate energy losses in the inverter, part (5) in Figure 3.B. The six power-electric switches that chop input DC to produce three phase AC will lose some power to parasitic resistance and their snubber circuits with every on-off cycle. Information pertaining to these losses was obtained from the datasheet of an appropriate model switch (Powerex 2009), including parasitic on-state resistance and switching energy loss as a function of off-state voltage difference and on-state current.

Switching frequency is the product of the desired motor input frequency and carrier wave frequency. The sum of the switch losses for every switch cycle multiplied by switching frequency gives the total loss power of the inverter, as shown in Figure 3.H.

Running maximum checks are performed for the electrical power supplied by the inverter and the current through it. These values assist with appropriate selection of inverter components.

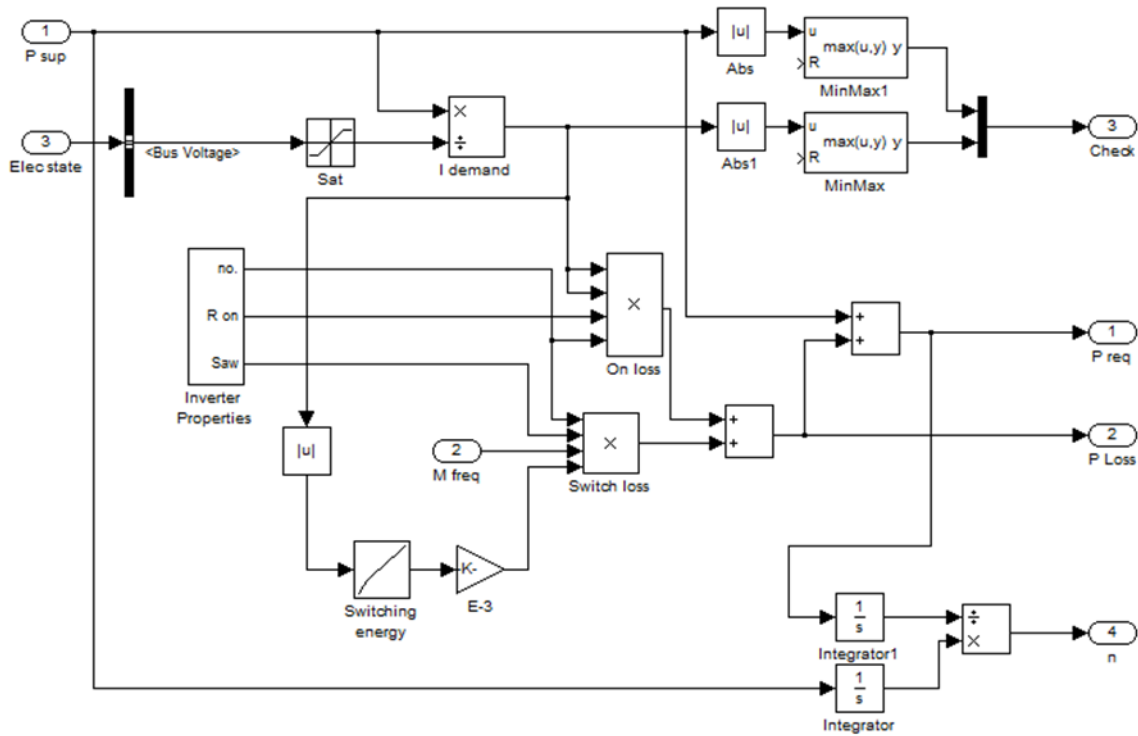


Figure 3.H - Inverter schematic

3.2.7 DC Converter

Figure 3.I shows an overview of the DC-DC converter subsystem, which may be explained in three parts: boost ratio calculation, energy management system, and losses. Boost ratios and losses form part (6) in Figure 3.B while EMS is part (7). Boost ratios are simply the ratios of the desired system bus voltage to the source voltages. The ratio of voltages indicates the ratio of demand current and current delivered from each source. As the voltage of a source decreases, the current required to maintain equivalent power increases.

The energy management system is responsible for allocating current demand across the two input sources; it is modelled as a subsystem of the DC-DC converter and shown in Figure 3.J.

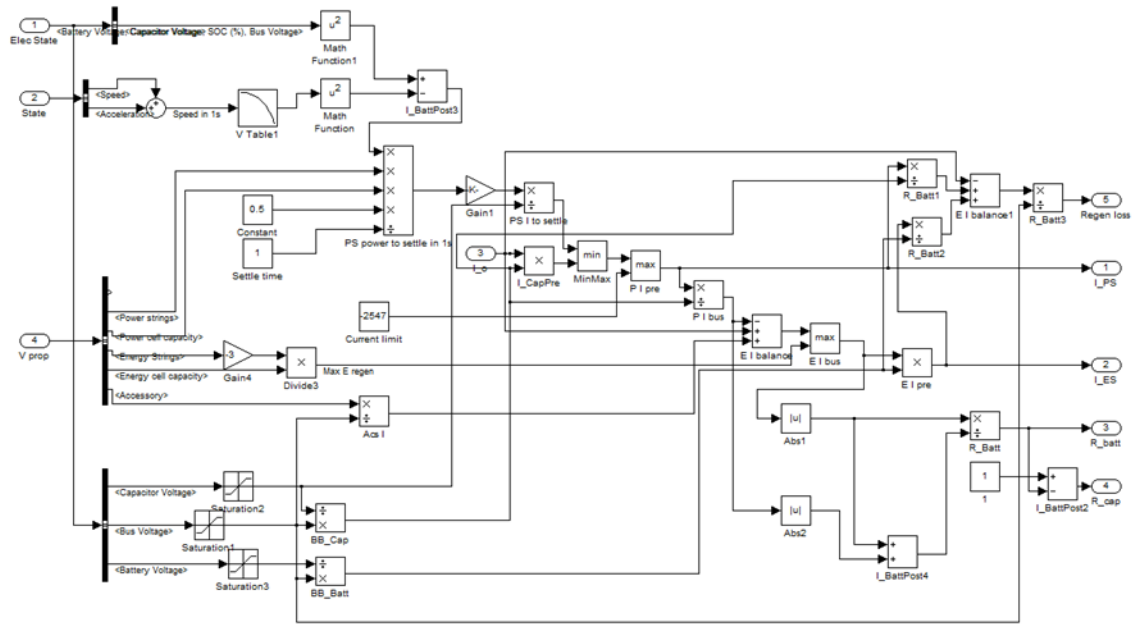


Figure 3.J - Energy management system schematic

Present vehicle speed and acceleration are used to estimate the vehicle speed one second into the simulation time. This speed is used as input to a lookup table that returns the desired state of charge of the power storage system, also one second from simulation time. The difference between this future desired SoC of the power system and its actual present value are compared, and the power output from or to the power system required to reduce this difference to zero is found. The power system outputs either this power (scaled by 0.33 to avoid overshoot and power system instability,) or the full demand power, whichever is less, subject to current delivery limitations. The difference between actual vehicle demand and the output of the power system is applied to the energy storage system. The scheme can mean that the energy system must supply more power than the vehicle demand, to charge the power system and bring it to the desired SoC for the present vehicle speed.

Estimating the DC-DC converter energy losses requires detailed knowledge of its power inductor. While inductors are available in a variety of off-the-shelf formats, it is uncommon to find components that are well suited to specific high voltage, high power applications. To accurately model the operation of the

DC-DC converter, an inductor was designed specifically for the purposes of the Pacifica's hybrid storage system conversion requirements.

The inductor was designed following the procedure presented by (McLyman 2004) for a gapped inductor using the core geometry approach. The final design uses four standard 180UI format inductor cores in parallel with a total inductance of 25 μH . Four cores are necessary to handle the current requirement, which is estimated to reach 1412 [A]. The core is designed to operate at a ripple frequency of up to 200 [kHz]. Complete design details of the inductor are presented in Appendix B.

Three types of energy loss in the DC-DC converter are dominant: (1) switching losses, similar to those in the inverter, (2) "copper loss" resulting from resistance in the windings of the inductor, and (3) "iron loss" in the inductor core due to magnetic hysteresis. All three are estimated empirically, within a subsystem of the DC-DC converter. This subsystem is shown in Figure 3.K.

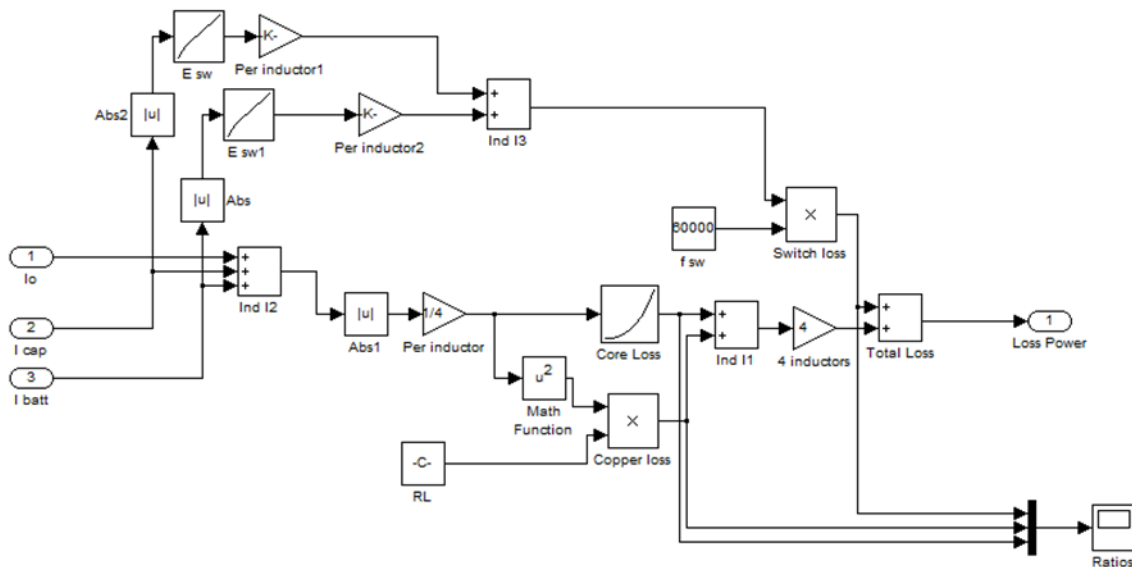


Figure 3.K - DC-DC converter loss schematic

Switching losses are determined in the same manner, and using the same model switch as for the inverter. Switching frequency is 60 [kHz], with one switch for each source. Current through each switch varies with power demand and off-state voltage varies with the voltage of its respective source. Copper losses

are determined from the total amount of current flowing through the inductor coils and the coil resistance. Iron losses are proportional to the amplitude of the ripple current in the coils, which is a fraction of the total current. Total current, I_T in the coils is the sum of the currents from each source, I_{S1} and I_{S2} , and the current delivered to the load, I_L .

$$I_T = I_{S1} + I_{S2} + I_L \quad (0-x)$$

Notice that the total current carried by the coils is double the current flowing through the device; this is a result of the switched nature of the DC-DC converter. As the voltage of either source decreases, more current must flow from that source to produce equivalent power. Thus, ripple current and iron loss vary with the SoC's of both sources.

Total energy losses are divided among the two input sources in a ratio equal to their instantaneous ratio of power delivery. The loss is expressed as a current at the system bus voltage, and fractions of this current are then scaled and added to each source current.

3.2.8 HESS

Both energy sources are represented within the HESS subsystem, using models under the SimPowerSystems blockset (The MathWorks, Inc. n.d.). These are part (8) in Figure 3.B. Models of lithium ion batteries and/or capacitors were used to represent the energy and power systems. To simulate demand, controlled current sources were used with inputs derived from the DC-DC converter subsystem. Rather than modelling complete banks of batteries or ultracapacitors, single cell models were used for both the power system and the energy system. Demand current of each cell was divided by the number of strings in its respective storage system, and output voltage multiplied by the stack height. The HESS subsystem is shown in Figure 3.L.

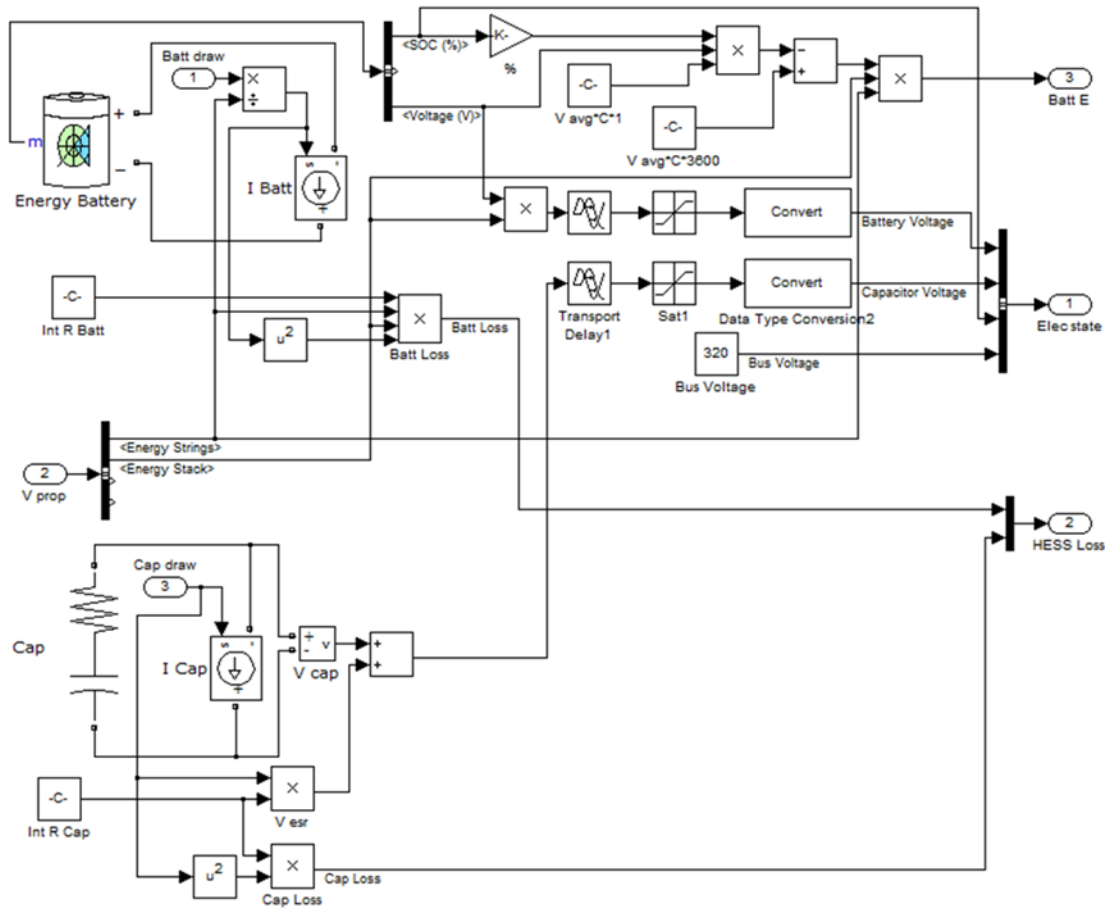


Figure 3.L - HESS calculations

The SimPowerSystems lithium ion battery model can be customized to match desired cell performance using a number of parameters. These parameters were adjusted to match the discharge profiles given in (Kokam Co. Ltd. 2010). A comparison of the modelled and actual discharge profiles is presented in Appendix C. A simple capacitor-resistor model is used to model an ultracapacitor with equivalent series resistance. In both cases, resistive energy losses by the storage system are calculated.

HESS calculation is dependent upon output from the DC-DC subsystem, which in turn requires feedback (voltage measurement) from the HESS subsystem. This establishes an algebraic loop that prevents Simulink from converging to a solution. The algebraic loop was resolved by adding a time delay of 0.5 [s] to the voltage measurements within the HESS subsystem. The time delay means that voltage can be explicitly

determined from its previous value instead of being implicitly dependent on its present value. The time delay was adjusted to the smallest value possible that did not result in anomalous voltage measurements.

3.3 Validation

To validate results obtained from the model powertrain, the model's parameters were adapted to suit those of a 1997 Chevrolet S10 Electric. The S10 Electric uses a single string of 26 lead acid batteries with a total bank voltage of 312 [V] (EV America, United States Dept. of Energy 1997). The S10 has a rated energy efficiency of 292 [Wh/mile] during the SAE J1634 drive, which equates to 181 [Wh/km]. The SAE J163 drive cycle consists of UDDS followed by HWYCOL.

A simulation of the vehicle in PSAT by Qin for the UDDS drive cycle results in energy usage of 182 [Wh/km] in the same drive cycle (Qin, Ms. 2009). Results from the model presented here indicate energy usage of 179 [Wh/km]. The results are in good agreement, with a difference of only 1.1% between the rated efficiency and the results of this powertrain model.

4.0 Results

In this section, observations from the study are presented and implications are discussed. Limitations of the modelling/simulation process are also summarized.

4.1 Scenarios

With a view to understand the trends and relations among hybrid storage system size and usage style, several scenarios have been tested. The scenarios include varying type of drive cycle, energy storage system, and storage system size. Details of these three dimensions are discussed in this section.

In each scenario, the energy use of the vehicle was measured and the range of the vehicle was predicted. Statistics relating to the energy system demand variation are recorded as a proxy metric for service life. These include the mean, standard deviation, minimum and maximum of current demand per battery cell in the energy system.

4.1.1 Energy Storage Systems

Design of the storage systems follows a kinetic energy based strategy described in section 3.1.2 - Hybrid Energy Storage Design Strategy. This section specifies two power systems based on ultracapacitor and ultra high power batteries. Three categories of storage system have been investigated here; (1) an energy dense battery system coupled with a capacitor power system, (2) an energy dense battery system coupled with an ultra high power battery system, and (3) a traditional, battery-only system as a control. Three sizes for each system have been specified: small (approximately 0.13 [m³]), medium (approximately 0.22 [m³]) and large (approximately 0.3 [m³]). The Pacifica's fuel tank capacity is much smaller, about 87 [L], or 0.087 [m³] (Allpar 2010). The only difference among the system sizes is the number of strings of batteries in the energy system. Detailed parameters of all battery models used in this study are given in Appendix D.

To provide a basis for comparison, the volume of all components in the storage system was kept as equal approximately among different storage systems in each size category. Details of the battery packs are summarized in Table 4.1. Note that a battery-capacitor system in the small size did not satisfy the

requirements for continuous running power: with the constant volume constraint, there would be too few energy batteries in the system to sustain highway cruising. This system was not tested.

Table 4.1 - Energy storage systems under consideration for Pacifica conversion

	Cell type	Strings	Stack height	Stack voltage [V]	Bank capacity [kWh]	Bank mass [kg]
Battery only						
Large	High power battery	7	84	354	69.6	647
Medium	High power battery	5	84	354	49.7	462
Small	High power battery	3	84	354	29.8	277
Battery-Capacitor						
Large	High capacity battery	35	84	354	69.6	441
	ultracapacitor	1	120	324	0.61	112
Medium	High capacity battery	21	84	354	41.8	265
	Ultracapacitor	1	120	324	0.61	112
Small	High capacity battery	7	84	354	13.9	88
	Ultracapacitor	1	120	324	0.61	112
Battery-Battery						
Large	High capacity battery	42	84	354	93.5	592
	Ultra high power battery	1	84	354	0.67	19
Medium	High capacity battery	33	84	354	65.6	416
	Ultra high power battery	1	84	354	0.67	19
Small	High capacity battery	21	84	354	41.8	265
	Ultra high power battery	1	84	354	0.67	19

4.1.2 Drive Schedules

Five drive cycles were introduced in section 2.0 - Vehicle Power Requirements. These five cycles, UDDS, LA92, US06, HWYCOL and NYCCCOL, include examples of travel in highway conditions, dense city traffic, and mild, moderate and aggressive urban use. Together they cover a wide gamut of typical conditions and so these five are used as separate cases in this study. Considering a range of driving conditions helps to highlight the performance of energy storage systems in different contexts.

4.1.3 Simulation Matrix

The range of storage systems tested and the drive cycles with which they are tested represent the simulation matrix. This is summarized in Table 4.2 with code names for each scenario.

Table 4.2 - Simulation matrix

	UDDS	LA92	US06	HWYCOL	NYCCCOL
Battery only					
Large	B.L-1	B.L-2	B.L-3	B.L-4	B.L-5
Medium	B.M-1	B.M-2	B.M-3	B.M-4	B.M-5
Small	B.S-1	B.S-2	B.S-3	B.S-4	B.S-5
Battery-Capacitor					
Large	BC.L-1	BC.L-2	BC.L-3	BC.L-4	BC.L-5
Medium	BC.M-1	BC.M-2	BC.M-3	BC.M-4	BC.M-5
Small	Not tested				
Battery-Battery					
Large	BB.L-1	BB.L-2	BB.L-3	BB.L-4	BB.L-5
Medium	BB.M-1	BB.M-2	BB.M-3	BB.M-4	BB.M-5
Small	BB.S-1	BB.S-2	BB.S-3	BB.S-4	BB.S-5

4.2 Results

In this section, findings are presented and discussed.

4.2.1 Range and Energy Efficiency Estimation

For each scenario, a model Chrysler Pacifica was simulated undergoing a drive cycle twice; once with the energy storage batteries at 100% charge, and once with the energy storage batteries at 30% charge. Each measurement for each scenario is the average of values taken from the 100% and 30% charge simulations. Averaging measurements between 100% and 30% accounts for differences in storage level voltage which increases conversion requirements and ohmic losses.

Each storage system within the three size levels have roughly equal volume, but different mass. It is appropriate to consider the driving range of a storage system against its mass. Figure 4.A shows the storage system mass and vehicle range achieved by each storage system. Points on this graph indicate the expected driving range assuming an equal proportion of driving in each of the five drive cycles. The vertical bars indicate the minimum and maximum expected range for each storage system.

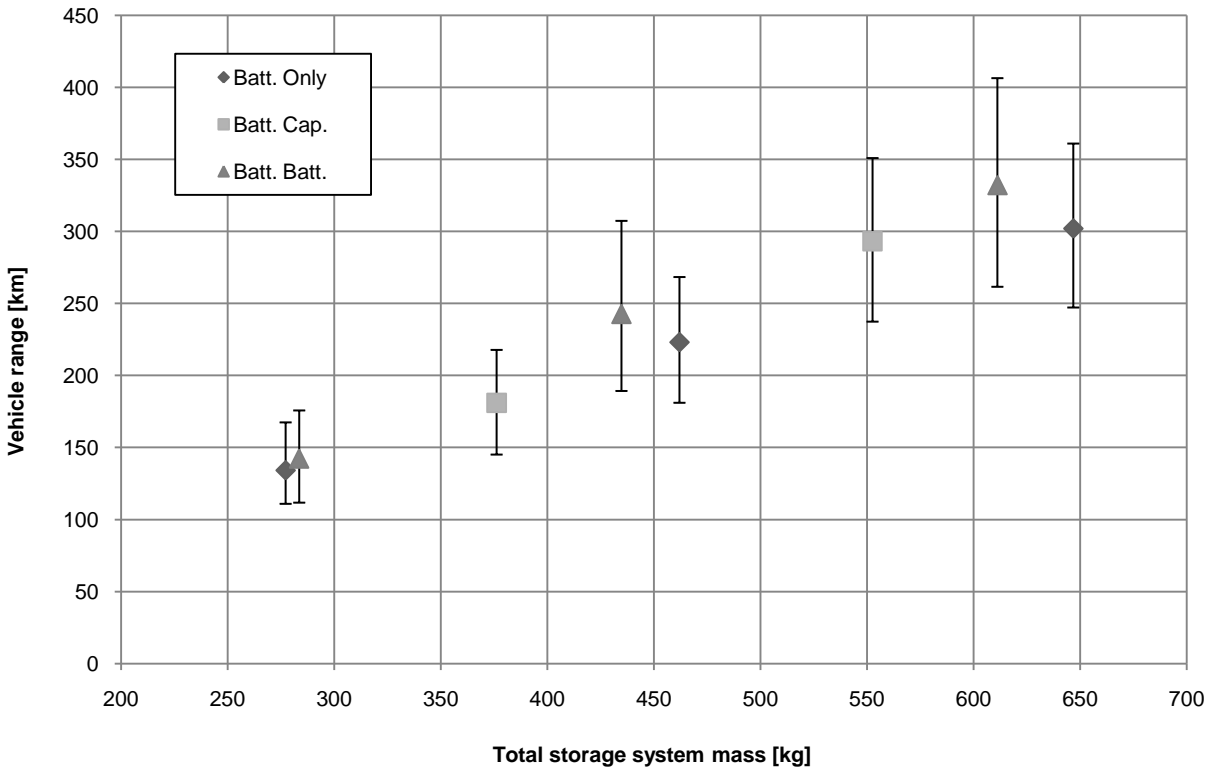


Figure 4.A - Range vs. storage system mass

Compared to the control scenario of simple power batteries, hybrid storage introduces four competing effects with respect to vehicle range: (1) increased energy density in the type of storage batteries used, leading to increased range, (2) more uniform current demand from the batteries, leading to increased range, (3) reduced volume available for energy batteries, leading to reduced range, and (4) differences in energy usage throughout the powertrain, with unpredictable results. Differences in energy usage arise in the form of losses within the storage system itself, voltage conversion losses, and changes to vehicle running requirements due to storage system mass. The data indicate that hybrid storage systems are lighter than battery-only systems at all size levels, and this is favourable in and of itself.

While battery-battery systems have greater vehicle range than the control, battery-capacitor systems have less. Given that both the large battery-capacitor and battery-only systems store equal amounts of energy (69.6 [kWh] each), the difference in range at this size must be due to increased losses within the storage system and the DC-DC converter. At the medium size, the battery-capacitor system has less energy capacity

than the control system (41.8 vs. 49.7 [kWh] respectively), meaning the dominant effect is that of reduced volume available for energy storage batteries. Indeed, the range penalty for the medium size battery-capacitor system is much larger than at the large size; a difference of 42 vs. 5 [km] respectively.

The power system within battery-battery systems occupies a much smaller volume of the total storage system than that of battery-capacitor systems. The result is increased energy capacity compared to the control at all sizes, with the gap increasing for larger system sizes. This, and the lighter weight of battery-battery compared to the control systems, explains the advantage in range they have over battery only systems.

Figure 4.B shows the same data as Figure 4.A, arranged here with respect to drive cycle. Recall that UDDS, LA92 and US06 represent mild, medium and aggressive urban driving respectively, while HWYCOL and NYCCCOL represent highway cruising and heavy congestion driving respectively.

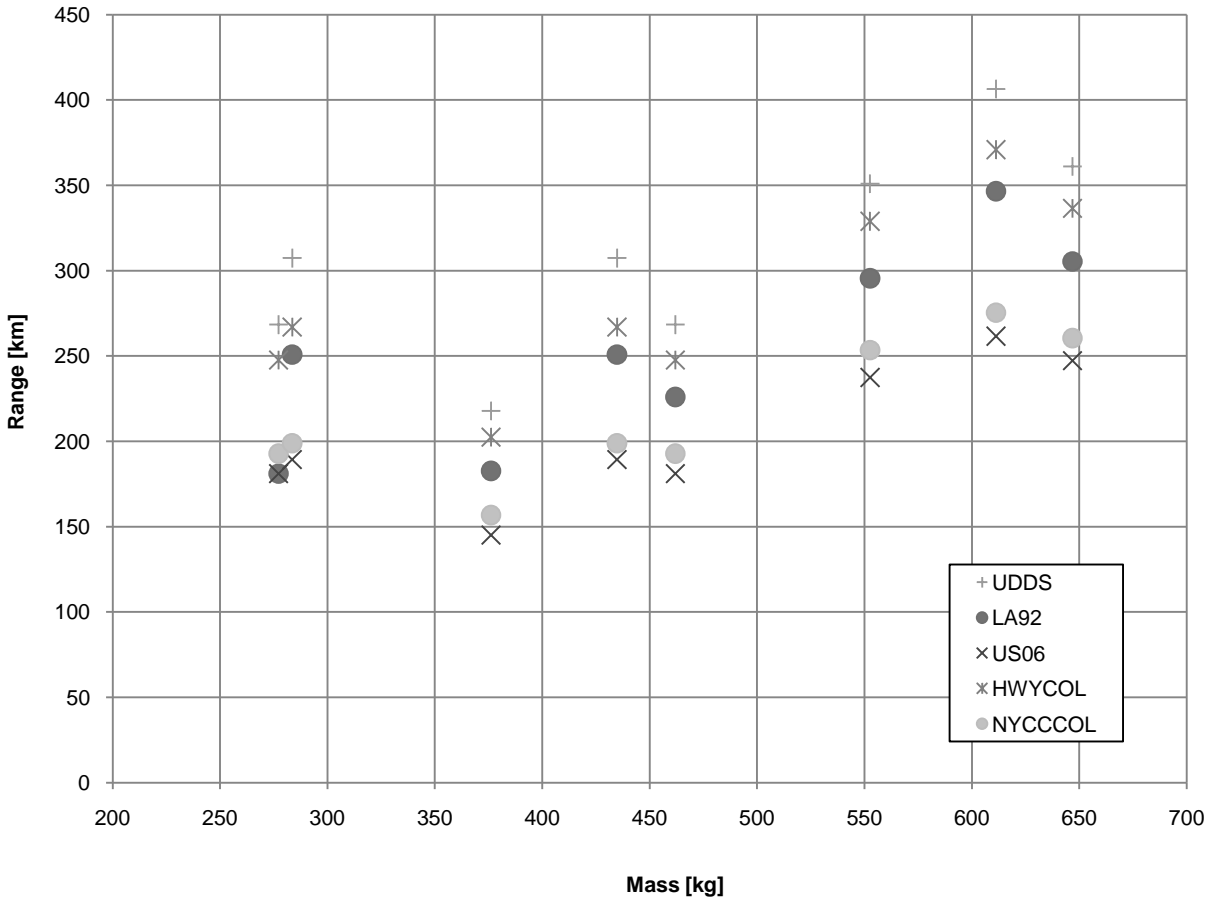


Figure 4.B - Range vs. mass per drive schedule

The data is mostly consistent; the most aggressive drive cycle, US06 results in the lowest range for all scenarios. An unexpected close second is the heavy traffic cycle, NYCCCOL. The poor energy efficiency of this cycle results from the low speed and average demand torque of the electric motor, which operates inefficiently in this range. LA92 results in a range close to the average of the five drive cycles tested aside from in one scenario corresponding to a small battery-battery system, where the range of this cycle is comparable to that of US06. The cause of this phenomenon is not understood, but the result is repeatable. The spectrum of vehicle range is observed to increase with increasing storage system size.

As mentioned previously in this section, energy usage and losses of the powertrain vary with each storage system. Measurement of energy usage is necessary to understand differences in vehicle range amongst

the different storage systems. Energy use and loss within the hybrid energy powertrain can be accounted for in eight categories:

1. Cruising - the energy required to overcome drag due to aerodynamic and rolling resistance
2. Motor losses - inefficiencies of the induction machine, whether as a motor or generator
3. Inverter losses - inefficiencies of the inverter
4. Converter losses - inefficiencies of the DC-DC converter
5. Energy losses - energy losses within the energy storage system
6. Power losses - energy losses within the power system
7. Accessory load - energy spent by air conditioning, exterior lighting, driver instrumentation, etc.
8. Regenerative losses - the difference between the amount of energy available to the storage system from decelerating the vehicle and the amount actually recovered

Note that in an ideal electric powertrain, the acceleration energy would be balanced by the regenerative energy collected by decelerating. As such, the energy required to accelerate the vehicle is not accounted for in its own category. The difference between acceleration energy and deceleration energy is accounted for among motor, inverter, converter and storage losses. In the case that limitations of the storage system prevent it from capturing all of the deceleration energy, the difference between the energy available to the storage system and the amount actually recovered is measured as a regenerative loss. Regenerative losses were not present in any of the scenarios tested here, and so this loss category has been dropped from consideration for this study.

Energy measurements in each of the remaining seven categories were recorded for all scenarios. Each measurement is the average of measurements taken from a drive cycle starting with the energy system at 100% and 30% charge. Energy usage is shown in Figure 4.C and Figure 4.D for the UDDS and US06 drive cycles respectively. Similar figures for the LA92, HWYCOL and NYCCCOL cycles are included in Appendix E.

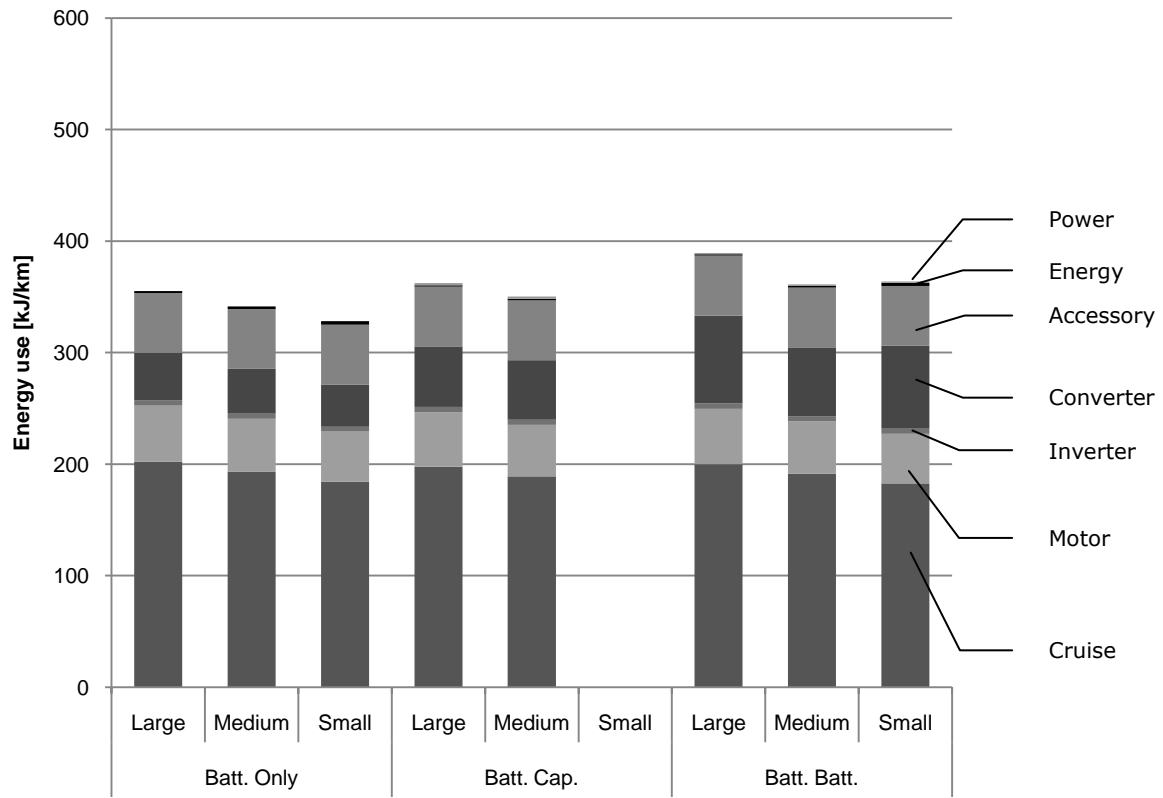


Figure 4.C- Energy usage breakdown for UDDS

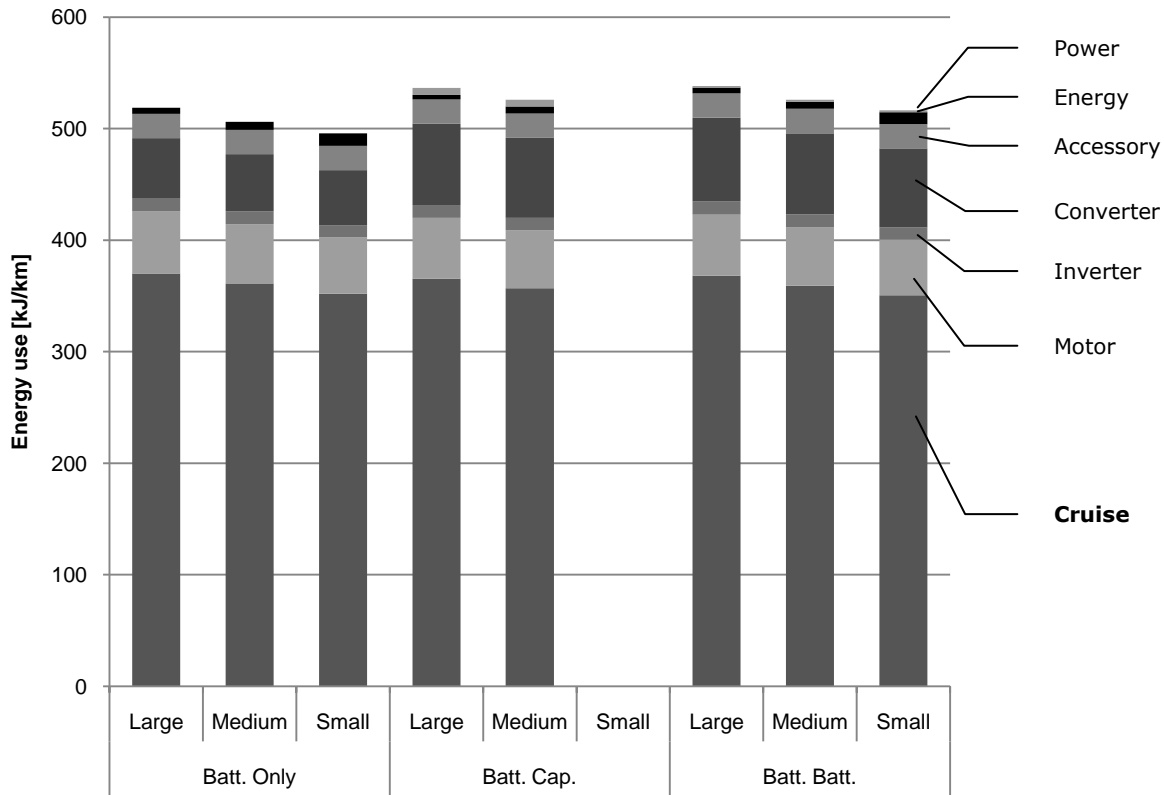


Figure 4.D - Energy usage breakdown for US06

The data indicate that energy usage increases with increasing storage system size, and that the increase is due to cruising energy; a heavier vehicle experiences increased rolling resistance. While cruising requirements increase with system size, energy losses decrease. As the storage system becomes larger, demand current is spread among more cells, reducing ohmic losses. Also noteworthy is that all of the hybrid storage systems have increased energy usage per [km] than the control does; this difference being mostly due to a difference in DC-DC converter requirements, but partly due to increased energy and power system losses as well. Among the hybrid storage systems, power losses increase with system size; the effects of increased mass are borne by the power system when accelerating the vehicle. Note that the battery-only system has no power losses since it has no power system.

Overall energy usage is much higher for the US06 cycle than for UDDS. This is expected, since US06 represents a much more aggressive driving pattern. The biggest increase in requirements between US06 and UDDS is in cruising energy, a result of much higher average speed in US06. Energy and power system losses,

converter, and inverter losses are all higher in US06 due to increased demand. Accessory usage per [km] is higher for UDDS; since accessory usage is a constant power load, accessory energy increases with time. A slower average speed means accessory usage per [km] is higher.

4.2.2 Service Life Effects

Accurately measuring the effects of different usage patterns on the service life of a battery requires destructive physical testing. Since service life is dependent upon, among other things, the amount of variation in demand current and the presence of current reversals, these factors are proxies that can be used to imply changes in battery service life.

Normalized current demand represents the current demand per battery cell within the energy system. Approximating this as a normal distribution, statistics of demand can be analyzed. Figure 4.E and Figure 4.F show the minimum, maximum, as well as the range of the mean of normalized demand plus and minus one standard deviation, or 68% confidence interval for the US06 and UDDS drive cycles, respectively. Similar figures are included in Appendix F for the remaining three drive cycles.

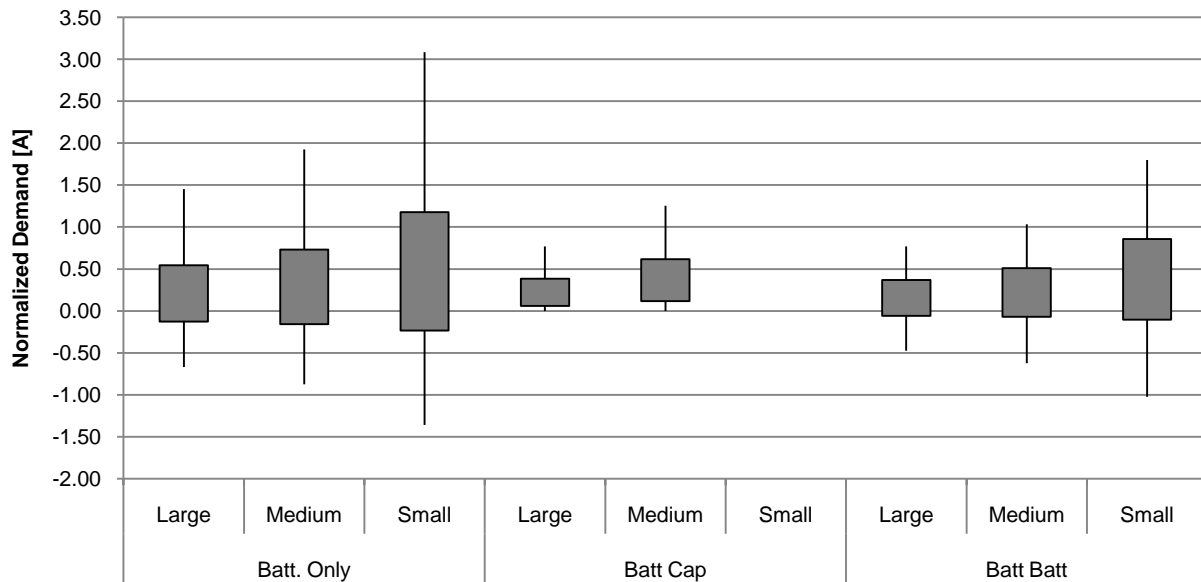


Figure 4.E - Normalized current demand for US06

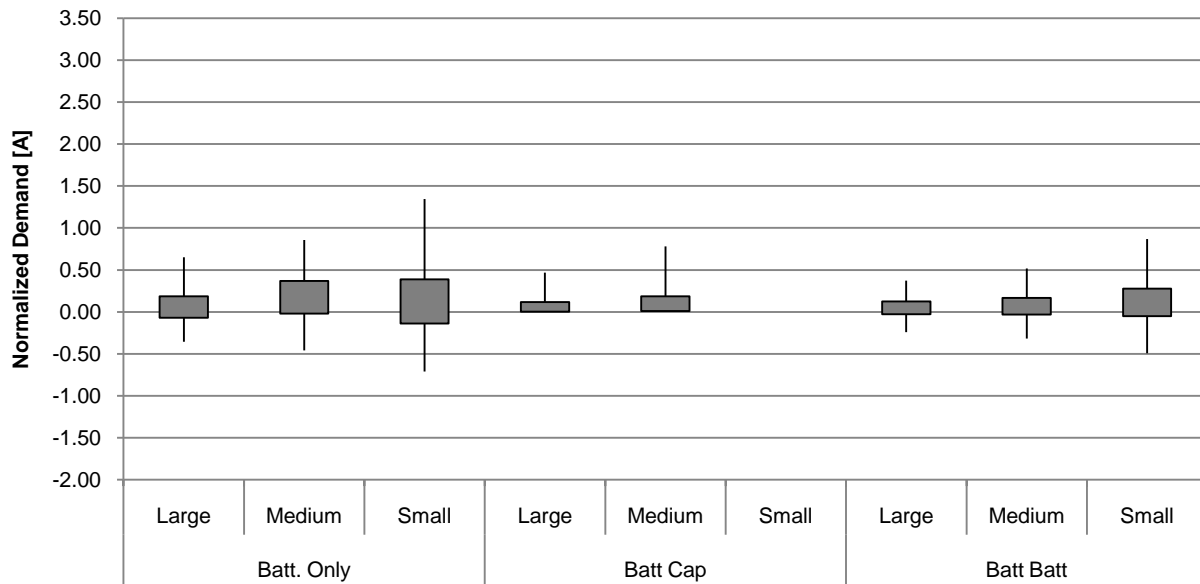


Figure 4.F - Normalized current demand for UDDS

Predictably, the maximum demand per cell is farther from the mean than the minimum is in all cases. While accelerating, drag forces increase the power required to change the vehicle's velocity, whereas they decrease the power required to decelerate the vehicle.

As expected, hybrid storage systems have a much narrower range and confidence interval than the control, indicating that the inclusion of a power system positively reduces the fluctuation of normalized demand for the energy batteries. The effect is stronger for batter-capacitor systems than for battery-battery systems. The implications to service life for battery-capacitor systems are made stronger by the fact that no negative demand is present at all, proving a lack of any current reversals. While current reversals are present for battery-battery systems, they are not as severe as for battery only scenarios.

Particularly for the US06 cycle, average demand is higher for battery-capacitor systems than for battery-battery systems. This is a result of the battery-capacitor system having fewer cells than the battery-battery systems. Average demand and demand variation can be seen to increase with storage system size in all scenarios.

Both average demand and variation increase for the US06 cycle compared to UDDS, this is expected given the higher accelerations and decelerations in US06. Furthermore, it appears that variation in the positive and negative sense increase in equal proportion.

4.2.3 Implications

It is apparent from the results that several tradeoffs lie in the choice of storage system, and the powertrain specifications. It follows that storage system design is application dependent, and that thorough consideration should be given to a vehicle's intended use in specifying a powertrain.

One factor that is expected to have an effect on storage system performance is the voltage bus. No variation in voltage bus was examined in any of the scenarios here. A higher bus voltage will have implications for the ohmic losses in the inverter, as well as switching energy losses in the converter and inverter.

A major implication of the findings here are that there is substantial scope for optimizing the storage system and powertrain design. The most significant parameters to be optimized are (1) bus voltage, (2) stack height of the energy system, (3) number of strings in the energy system, (4) stack height of the power system, and (5) number of strings in the power system. At a component level, the increased losses in the DC-DC converter for both hybrid storage systems suggest that converter design is crucial to hybrid storage system success. An improved design may reduce or eliminate the difference in conversion losses.

In all cases, a larger energy storage system leads to less demand on its components and lower ohmic losses within the storage system, but greater overall energy consumption per [km] due to increased vehicle mass. The effect of the size of the power system has not been investigated here. With both hybrid storage systems, the advantage over the battery-only system improves as the system size increases. This suggests hybrid storage systems are most appropriate at large system sizes, particularly for battery-capacitor systems.

In the case of a battery-capacitor system, a larger power system is not expected to have any marginal benefit, since the existing system already has enough capacity to contain the kinetic energy of the vehicle at

highway speed. A smaller power system would lead to increased space with which to add more energy batteries. This would lead to longer vehicle range and reduced demand per cell, but may result in the power system not having sufficient capacity to fully sustain vehicle acceleration or regenerative braking. This would lead to larger demand variation for the energy batteries and possibly some current reversals as well.

In the case of the battery-battery system, changing the size of the power system is more complicated. The capacity of the system can be adjusted by increasing or decreasing the SoC window, so removing batteries from the power system wouldn't necessarily cause a lack of capacity for acceleration. A smaller battery power system would result in less ability to absorb regenerative braking, since a lower stack has a lower voltage and would have to accept more current from the DC-DC converter to absorb the same power. The power system is already current-limited in regeneration with the current configuration.

For comparison, the overall system energy and power densities are plotted on the same Ragone plot as in section 2.3.3 - Comparison of Storage Technologies, together with the batteries and capacitors. This plot is shown in Figure 4.G.

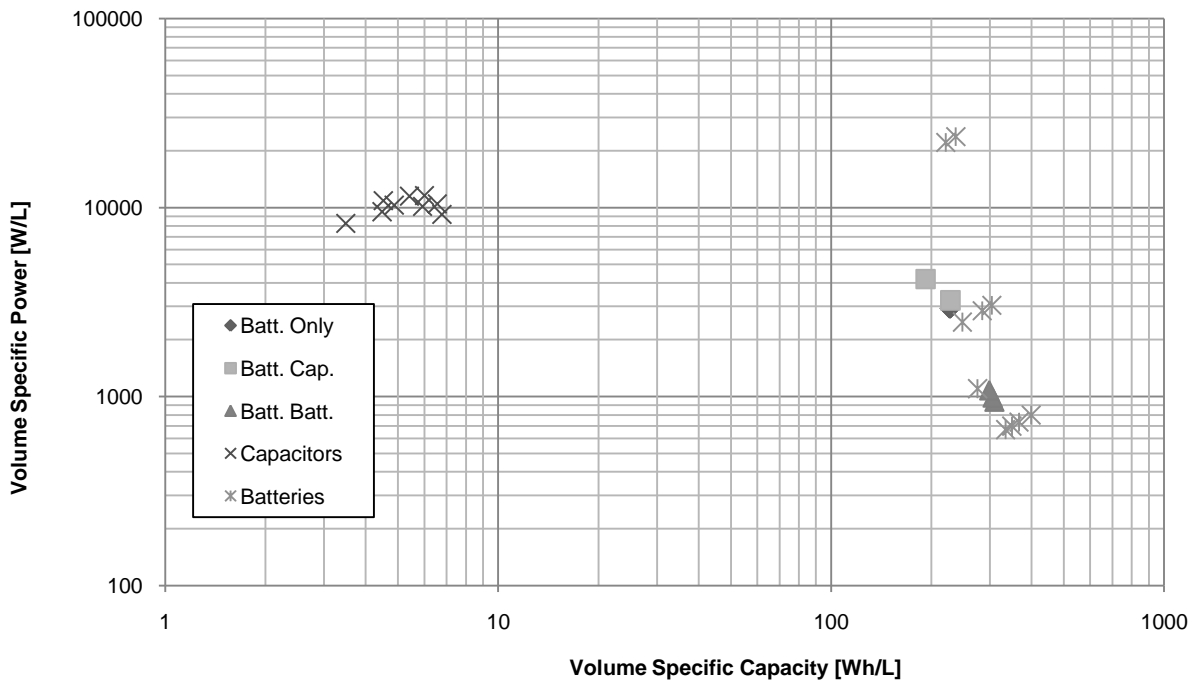


Figure 4.G - System volume specific power vs. volume specific capacity

That there are some battery cells in Figure 4.G with higher energy and power density than the ultracapacitor systems deserves some discussion. It should be noted that the values depicted in Figure 4.G represent peak output. This peak output is duration limited, and is not necessarily the same as peak input. In the case of the ultra-high power batteries, which appear to be similar to battery-capacitor systems in Figure 4.G, this peak output is limited to 10 [s] duration. Furthermore, the peak input of these batteries is much less than peak output. This has important consequences for storing regenerative braking energy, one of the key functions these batteries are to perform. In the case of battery-capacitor systems, the capacitor peak output is limited by the energy content of the capacitors, and input power is equal to output power.

As stated in section 2.3.3 - Comparison of Storage Technologies, no single electrical storage device exists that makes a mid-way compromise between the power density of capacitors and the energy density of batteries. Hybrid storage systems can be designed to fill a space anywhere in this gap as appropriate.

4.3 Limitations

This study is intended to develop a basic understanding of hybrid energy storage systems in the context of a passenger vehicle; specifically, the Chrysler Pacifica. The study is not a comprehensive review of hybrid electric storage systems in general, nor is it fully sufficient to understand the implications hybrid storage systems within the context of the Pacifica, or to implement such a storage system. This section provides a discussion of the limitations of this study.

4.3.1 Simplification and Approximation

A key limitation of the study is that it involves no physical testing. The results of a modeling/simulation approach are highly dependent on the quality of modeling and simulation. A perfect model is often unattainable owing to incomplete information, overload of detail, or computational expense. Often these problems are addressed with appropriate simplifications or approximations. For the purposes of this study, a fully switched electrical model of the inverter, converter and induction motor were much too computationally expensive to be able to simulate the powertrain's operation for the range of 600 - 1500 [s] as is required to simulate the drive cycles. This problem was solved by simplifying the motor to an efficiency lookup table, and

modeling energy loss within the inverter and DC-DC converter with empirical relationships. While every effort was made to make the motor efficiency lookup table accurately reflect a real motor's characteristics, this can only be confirmed against physical testing of the motor, the data for which was unavailable for this study.

An approximation had to be made for the batteries' internal resistance, a parameter that is generally considered proprietary, confidential information. A value was suggested by Simulink's battery model generator based on the type of battery, capacity, nominal discharge rate, etc. This value was selected since better information could not be found at the time. The Simulink battery model does not account for the Peukert effect (MathWorks 2010), which is an important limitation since one of the expected advantages of hybrid storage leverages the increased useful capacity of a battery when depleted at a slower rate.

4.3.2 Drive Schedule

The drive schedules used in this study are widely used in studies of vehicle powertrains, but do not contain complete information. The drive cycles consist of velocity data at one second intervals, but have no information about road corners, surface, gradient, weather conditions, use of vehicle accessories, etc. Several such factors beyond the velocity profile can affect the energy consumption of the vehicle. In the absence of this information, it is assumed that the vehicle travels in a straight line over level terrain with no wind and with a constant, estimated accessory load.

It is significant that the drive cycles here are selected to cover a wide variety of common vehicle usage; they are no more a comprehensive representation of general human driving behaviour than a single person is representative of the entire human population. Idiosyncrasies vary widely among the driving population, among other things changing with geographic location, age, and gender. Completely covering all possible driving scenarios is impossible, and the best available alternative is to use the drive cycles that are the most widely used for other powertrain studies.

4.3.3 Hybrid Control Scheme

The hybrid control scheme used in this study to allocate power demand across the batteries and ultracapacitors is attractive in its simplicity and derivation from the basic concept of kinetic energy. It is, however, substantially less complicated than other similar schemes of its kind (Jalil, Kheir and Salman 1997), (Lukic, et al. 2006), (Rossario, et al. 2006). While the scheme generally performed fine for all the scenarios observed here, driving situations that involved rapid oscillations of acceleration and deceleration could cause it to behave in a somewhat unstable fashion. Furthermore, it was better suited to the operation of the ultracapacitor based HESS than the battery-battery system. The control should be more thoroughly optimized for the system it is paired with.

4.3.4 Battery Service Life

As discussed in section 4.2.2 - Service Life Effects, actual implications of a hybrid energy storage on battery service life are very difficult to determine without physical, destructive battery cell testing. The closest and most readily understood proxy to measuring service life is to measure the fluctuation of current demand on each cell, and the degree of current reversal. While these metrics can be used to imply an improvement in battery service life, they cannot be used to guarantee it, or to measure it.

4.3.5 Chapter Summary

In this chapter, results are presented from the testing described in section 3.0 - Vehicle Configuration and Simulation. It is shown that the control, battery-only systems, are heavier in most cases than any of the hybrid systems. Further, it is shown that a battery-capacitor system has advantages over both the control and the battery-battery systems in mass and expected service, while battery-battery systems provide increased range at decreased mass in most cases, while making a large improvement in expected service life compared to battery-only systems.

The results found here are mostly agreeable to the findings of Hoelscher, et al, who also found that battery-capacitor systems decreased mass and improved service life. Hoelscher however, found that hybrid energy system had reduced internal resistance losses compared to battery-only systems, whereas this study

measured a slight increase. Hoelscher's 2006 paper did not provide results pertaining to battery-battery systems.

5.0 Conclusions and Recommendations

This section covers conclusions of section 4.0 - Results, and recommendations that follow from those conclusions.

5.1 Conclusions

The objective of this study was to evaluate the effectiveness of a hybrid electric energy storage system for use in a modified Chrysler Pacifica. The results show that effectiveness of a hybrid storage system depends on the size and type of the hybrid storage system, the type of driving patterns observed, and what metrics are evaluated. The results are conclusive to the extent that the model and simulation of the modified Pacifica powertrain are accurate.

Hybrid storage can successfully be used to reduce vehicle mass, as well as demand variation and current reversals of the energy system battery cells. The reduction in demand variation and current reversals implies a longer service life for these battery cells. Reduction of mass, demand variation and current reversals was greatest in battery-capacitor systems. A battery-battery HESS improves total energy capacity for all system sizes tested, while a battery-capacitor HESS increases energy capacity only for the largest system size tested here, with approximately 70 [kWh] of storage.

Although energy capacity is improved in most HESS's tested here, energy consumption is increased. The increase comes predominantly in higher DC-DC converter losses, demonstrating that hybrid energy storage has implications for other components in the powertrain.

The power system of the battery-battery HESS was unable to fully accommodate regenerative braking demand in all cases, resulting in some current reversals for the energy batteries. This leads to the conclusion that a battery-capacitor system is appropriate for applications demanding frequent, large velocity changes. The power system of the battery-capacitor HESS was very bulky, limiting space for energy batteries. This reduced vehicle range compared to the battery-battery system, leading to the conclusion that a battery-battery system is appropriate when range is the primary concern.

Given the intricate set of compromises between the size and makeup of the storage system, the bus voltage, and converter design, it is apparent that optimization is required to realize the full potential of a

HESS. Successful optimization will determine the best makeup of any given class of storage system to best achieve a given set of design objectives and lead to the greatest energy capacity, power capacity and energy efficiency of the system that is possible given a set of constraints.

5.2 Recommendations

The foremost recommendation in the design of a HESS is to employ genetic algorithms or other form of optimization to find the optimum bus voltage and numbers of energy and power strings and stack heights in the storage system. Optimization should be application specific, with design objectives defined such that the system is tailored to the intended use of the vehicle. For instance, HESS optimization for a vehicle that is expected to experience frequent velocity changes should favour a battery-capacitor solution, whereas a vehicle intended for long distance driving should favour a battery-battery system.

A second recommendation is to carefully consider the design of DC-DC converter for the application, with a view to minimizing losses. Reducing energy loss in the DC-DC converter will bring the efficiency of a HESS closer to that of a battery-only, improving range relative to these systems.

Thirdly, the control scheme should be optimized. In this study, the control scheme considered vehicle kinetic energy only. Fuzzy logic may be a suitable technique to apply to the control scheme as a means of considering kinetic energy and other factors as appropriate. For best results, the control scheme and optimization of the HESS parameters should be considered simultaneously.

To overcome the limitations of modeling and simulation in this study, it is suggested to perform physical testing. A prototype powertrain as well as battery testing can be used to corroborate the results found here. Battery testing using cycles corresponding to the usage patterns discovered here will lead to a better understanding of exactly how battery service life is affected by storage hybridization.

References

- Abuelsamid, Sam. "ABG Tech Analysis and Driving Impression: GM's HCCI Engine." *AutoBlogGreen*, 8 26, 2007.
- Allpar. *Allpar*. 2010. <http://www.allpar.com/model/pacifica-specs.html> (accessed 6 30, 2010).
- Argonne National Laboratory. *Transportation R&D Center*. U.S. Department of Energy. 2010. http://www.transportation.anl.gov/modeling_simulation/PSAT/index.html (accessed 7 5, 2010).
- Author, Unknown. "Building the S-10 Electric." *Automotive Manufacturing & Production*, 7 1997.
- . *Ecomodder*. <http://ecomodder.com/forum/emgarage.php?do=details&vehicleid=2257> (accessed 6 30, 2010).
- AVL. *AVL - ADVISOR*. AVL. 2010. <http://www.avl.com/wo/webobsession.servlet.go?app=bcms&page=view&nodeid=400030459> (accessed 7 5, 2010).
- Baisden, Andrew, and Ali Emadi. *ADVISOR-Based Model of a Battery and an Ultra-Capacitor Energy Source for Hybrid Electric Vehicles*. IEEE, 2004.
- Bryant, A.T., A. Walker, and P.A. Mawby. *Fast Inverter Loss Simulation for Hybrid Electric Vehicle Drives*. Coventry, UK: School of Engineering, University of Warwick.
- Buchmann, Isidor. *Part Two*. 2003. <http://www.batteryuniversity.com/parttwo-34.htm> (accessed 05 19, 2010).
- Cassio, T.C. Andrade, and S.T. Ricardo Pontes. *Three-Phase Induction Motors Energy Efficiency Standards*. Case Study, Ceara Federal University.
- Chan, H, and D Sutanto. *A New Battery Model for use With Battery Energy Storage Systems and Electric Vehicle Power Systems*. Hung Hom, Hong Kong: The Hong Kong Polytechnic University.
- Cho, Don-Hyeok, Hyun-Kyo Jung, and Cheol-Gyun Lee. "Induction Motor Design for Electric Vehicle Using a Niching Genetic Algorithm." *IEEE Transactions on Industry Applications*, *VOI 37, No. 4*, 2001: 994.
- Ciobotaru, M, T Kerekes, R Teodorescu, and A Bouscayrol. *PV Inverter Simulation Using MATLAB/Simulink Graphical Environment*. Aalborg, Denmark: Scientific Commons, 2008.
- Conway, B. *Electrochemical Supercapacitors*. New York, NY: Kluwer Academic / Plenum Publishers, 1999.
- Dodge, Onathan. "IGBT Tutorial Part 2 - Static, dynamic characteristics." *Industrial Control Design Online*. United Business Media, 3 13, 2007.
- Editors, Green Car Journal. "Could In-Wheel Motors be the Next Big Thing?" *Green Car*, 2010.
- Emadi, Ali. *Handbook of Automotive Power Electronics and Motor Drives*. Boca Raton: CRC Press, 2005.

EV America, United States Dept. of Energy. *1997 Chevrolet S-10 Electric Vehicle Specifications*. 1997.

General Motors Canada. *2011 Chevrolet Volt*. 2010.

<http://www.chevrolet.com/pages/open/default/future/volt.do> (accessed 6 30, 2010).

General Motors. *EV1 Specifications*. 2001. http://www.evchargernews.com/CD-A/gm_ev1_web_site/specs/specs_specs_top.htm (accessed 7 9, 2010).

Hilton, Jon. "What Has Formula 1 Ever Done For Us?" *SAE Congress 2010*. Detroit, Mi, (4 14, 2010).

Hodkinson, Ron, and John Fenton. *Lightweight Electric/Hybrid Vehicle Design*. Woburn: Butterworth-Heinemann, 2001.

Hoelscher, David, Alex Skorcz, Yimin Gao, and Mehrdad Ehsani. "Hybridized Electric Energy Storage Systems for Hybrid Electric Vehicles." *IEEE Power and Propulsion Conference*, 2006.

Hoffman, T, M Steinbuch, and R Druten. "Modeling for simulation of hybrid drivetrain components." *Vehicle Power and Propulsion Conference*, 2006.

Honda Motor Co., Ltd. *Honda IMA System/Power Unit*. 2010.

http://world.honda.com/CIVICHYBRID/Technology/NewHondaIMASystem/PowerUnit/index_1.html (accessed 7 1, 2010).

—. *Ultra-capacitor, The Honda FCX*. 2010. <http://world.honda.com/FuelCell/FCX/ultracapacitor/> (accessed 6 30, 2010).

Huang, Bufu, Zhancheng Wang, and Yangsheng Xu. "Multi-Objective Genetic Algorithm for Hybrid Electric Vehicle Parameter Optimization." *IEEE/RSJ International Conference on the Intelligent Robots and Systems*. Beijing: IEEE, 2006.

Jalil, Nashat, Naim Kheir, and Mutasim Salman. "A Rule-Based Energy Management Strategy for a Series Hybrid Vehicle." *Albuquerque: American Control Conference*, 1997.

Jinrui, N, and R Qinglian. *Simulation and Analysis of Performance of a Pure Electric Vehicle With a Supercapacitor*. Beijing, China: Beijing Institute of Technology.

Johnson Controls. "Hybrid Vehicle Technology." *Johnson Controls*. 2010.

http://www.johnsoncontrols.co.uk/publish/us/en/products/power_solutions/media_kit/sustainability/hybrid_vehicle_technology.html (accessed 6 30, 2010).

Kisacikoglu, M, M Uzunoglu, and M Alam. "Fuzzy Logic Control of a Fuel Cell/Ultra-capacitor Hybrid Vehicular Power System." *Vehicle Power and Propulsion Conference*, 2006.

Kokam Co. Ltd. "Product Catalogue." *Kokam America*. 2010.

http://www.kokam.com/english/product/battery_main.html (accessed 05 19, 2010).

Lachichi, A., and N. Schofield. "Comparison of DC-DC Converter Interfaces for Fuel." *IEEE Vehicle Power and Propulsion Conference*, 2006.

LeBlanc, John. "Tough Road Ahead for Electric Cars." *Toronto Star*, 4 3, 2010: W3.

Lin, C, et al. *Integrated, Feed-Forward Hybrid Electric Vehicle Simulation in SIMULINK and its Use for Power Management Studies*. Society of Automotive Engineers, 2001.

Lukic, S, and A Emado. *Modeling of Electric Machines for Automotive Applications Using Efficiency Maps*. Illinois: Illinois Institute of Technology.

Lukic, Srdjan, Sanjaka Wirasingha, Fernando Rodriguez, Jian Cao, and Ali Emadi. "Power Management of an Ultracapacitor/Battery Hybrid Energy Storage System in an HEV." *IEEE Power and Propulsion Conference* (IEEE Power and Propulsion), 2006.

Masrur, Abul, and Chris Mi. *Fundamentals of Hybrid Electric Vehicles Seminar*. SAE International, 2006.

MathWorks. *The MathWorks*. 2010. <http://www.mathworks.com/> (accessed 7 5, 2010).

McLyman, Colonel Wm. *Transformer and Inductor Design Handbook, 3rd ed*. Columbus, OH: Marcel Dekker, Inc, 2004.

Mendes, Christopher. *Torque Control Strategies for AWD Electric Vehicles*. Thesis, Waterloo: University of Waterloo, 2006.

Miller, John. "Accessory Overload Threatens Auto Power Budgets." *Automotive Design Online*. United Business Media, 9 20, 2006.

Montazeri-Gh, Morteza, Amir Poursamad, and Babak Ghalichi. "Application of Genetic Algorithm for Optimization of Control Strategy in Parallel Hybrid Electric Vehicles." *Journal of The Franklin Institute* (Elsevier), 2006.

National Highway and Traffic Safety Administration. *NHTSA*. 2010. <http://www.nhtsa.gov/#6> (accessed 7 1, 2010).

NESSCAP Co., Ltd. "NESSCAP Ultracapacitor Products." *NESSCAP*. 2008. http://www.nesscap.com/products_edlc.htm (accessed 05 19, 2010).

New-cars.com. *New-Cars.com*. 2004. <http://www.new-cars.com/2004/chrysler/chrysler-pacifica-specs.html> (accessed 7 27, 2010).

Odvarka, Erik, Abdeslam Mebarki, David Gerada, Neil Brown, and Cestmir Ondrusek. "Electric Motor-Generator for a Hybrid Electric Vehicle." *Engineering Mechanics*, 2009: 131-139.

Who Killed the Electric Car. Directed by Chris Paine. 2006.

Patrascu, Daniel. "Ford Focus Electric to be Built in Michigan." *AutoEvolution*, 1 12, 2010.

Perreault, David. "Course# 6.334 "Power Electronics" course notes." Boston: Massachusetts Institute of Technology.

Powerex. *CM200DU-12NFH*. Product Datasheet, Youngwood, PA: Powerex, Inc., 2009.

POWERSIM. *PSIM 9*. <http://www.powersimtech.com/> (accessed 7 6, 2010).

Qin, Helen, interview by Karl Mikkelsen. *Ms.* (04 21, 2009).

Qin, Helen, interview by Karl Mikkelsen. *Simulation of S10 in PSAT* (7 5, 2009).

Rizzoni, Giorgio, Lino Guzzella, and Bernd Baumann. *Unified Modeling of Hybrid Electric Vehicle Drivetrains*. IEEE, 1999.

Rossario, L, P Luk, J Economou, and B White. *A Modular Power and Energy Management Structure for DUal-Energy Source Electric Vehicles*. Shrivenham, UK: Cranfield University, 2006.

Russ, Carey. "2006 Chrysler Pacifica Touring AWD Review." *The Auto Channel*, 2006.

Samborsky, Steven. *Design and Simulation of an Ultracapacitor Based Hybrid Electric Vehicle*. Waterloo: University of Waterloo, 2006.

Sherman, Don. "Features: Technology of the Year: GM's Two-Mode Hybrid System." *Automobile*, 2 2009.

SmartGauge Electronics. *Smart Gauge*. 04 02, 2008. http://www.smartgauge.co.uk/peukert_depth.html (accessed 05 19, 2010).

Styles, Geoffrey. "What Peak Oil?" *Energy Tribune*, 6 25, 2010.

The MathWorks, Inc. *Asynchronous Machine, Simulink product documentation*. 2009.

Toronto. *2010 Toyota Prius*. 2010. <http://www.toyota.ca/cgi-bin/WebObjects/WWW.woa/7/wo/Home.Vehicles.Go.Prius-CtZRtmM7qZpzKUYlle1IXw/3.9?fmg%2fprius%2fintro.html> (accessed 6 30, 2010).

U.S. Dept. of State Office of the Historian. "OPEC Oil Embargo, 1973-1974." *Milestones*. <http://history.state.gov/milestones/1969-1976/OPEC> (accessed 7 1, 2010).

United States Environmental Protection Agency. *Testing and Measuring Emissions*. March 19, 2008.

Vetter, J, et al. "Ageing mechanisms in lithium-ion batteries." *Journal of Power Sources*, 2005.

Wang, Lingfeng. *Hybrid Electric Vehicle Design Based on a Multi-Objective Optimization Evolutionary Algorithm*. Texas A&M University, 2005.

Westbrook, Michael H. *The Electric and Hybrid Electric Car*. Stevensage: The Institution of Electrical Engineers and Society of Automotive Engineers, 2001.

Winkler, Dietmar, and Clemens Guhmann. *Hardware-in-the-Loop simulation of a hybrid electric vehicle using Modelica/Dymola*. Technical University of Berlin.

Wright, R, et al. "Power fade and capacity fade resulting from cycle-life testing of Advanced Technology Development Program lithium-ion batteries." *Journal of Power Sources*, 2003.

Xiaomin, Pu, Liao Chenglin, Wang Lifang, and Zhang Junzhi. "Test and Improvement of HEV Control Strategies Using PSAT." *IEEE*. Dearborn, MI, 2009.

Yalamanchili, Krishna, and Mehdi Ferdowsi. "New Double Input DC-DC Converters for Automotive." *IEEE Power and Propulsion Conference*, 2006.

Appendix A - Chrysler Pacifica Specifications

Chrysler Pacifica Feature Highlights

- Six-passenger Luxury Seating in Three Rows (2 + 2 + 2)
- Full-Length Center Console - 1st and 2nd Rows
- Seats - Power 10-way Driver, 4-way Passenger
- Power Adjustable Pedals with Memory
- Dual Zone Automatic Temperature Control
- Fold-Flat Load Floor
- Tire Pressure Monitoring System
- Next Generation (Multi-Stage) Front Air Bags*
- Three-Row Side Curtain Air Bags*
- 3.5-l, 24-Valve, SOHC V-6 Engine
- (250 Horsepower, 250 lb.-ft. Torque)
- Four-speed Automatic Transaxle with Autostick®
- On-demand All-wheel Drive or Front-Wheel Drive with Traction Control
- Four-wheel Antilock Disc Brakes
- (318 x 28 mm Front and 312 x 14 mm Rear)
- Five-link Independent Rear Suspension with Load-leveling and Height Control
- 17-inch P235/65 Tires and Aluminum Wheels

Standard Features

- Heated First- and Second-Row Seats
- Leather-Trimmed Seats
- In-Cluster Navigation System - INDUSTRY FIRST
- Infinity Intermezzo (TM) Digital 5.1 Surround sound
- UConnect Hands-Free Communication System (TM)
- DVD Rear Seat Video (TM) Entertainment System
- SIRIUS Satellite Radio (TM) Prep
- High-Intensity Discharge Headlamps
- Door-Mounted Front Seat Power Switches
- Power, Front & Rear One-touch Down Windows
- Power Locks
- Illuminated Keyless Entry with Central Locking
- Security Alarm System
- Sentry Key Theft Deterrent System
- Radio/Driver Seat/Exterior Mirrors Memory
- Universal Garage Door Opener System
- Sunglass Holder
- Illuminated Vanity Mirrors in Sun Visors
- Tachometer
- Power Accessory Delay
- 4 Power Outlets - Front & Rear
- Folding Second and Third Row Seats
- Rear Cargo Storage Bin
- Leather-Wrapped Shift Knob & Steering Wheel
- Steering Wheel-Mounted Audio Controls
- Speed Control
- Tilt Steering Column

- Instrument Panel Mounted Ignition Switch
- Climate Control Outlets - Front/Rear
- Air Filtering
- Solar Control Sunscreen Glass
- Rear Window Defroster
- Automatic Halogen Headlamps
- Fog Lamps
- Exterior Mirrors - Dual, Power, Heated Fold-Away with Auto Dim Driver
- Inside Rear View, Auto Dim Mirror
- Antenna - Integrated in Side Window
- Sound System: AM/FM Radio with Compact Disc and Changer Control with 150 watt amplifier and seven Infinity (R) speakers
- Rear Window Wiper/Washer
- Fuel Tank - 23 Gallons

Chrysler Pacifica Specifications

All dimensions are in inches (millimeters) unless otherwise noted

- Assembly Plant Windsor, Ontario, Canada
EPA Vehicle Class Multi-purpose vehicle
- Engine: 3.5-liter, 24-Valve, SOHC, SMPI V-6
 - Plenum intake manifold operated with electronically controlled manifold tuning valve and short-runner valves
 - Displacement 214.7 cu. in. (3518 cu. cm)
 - Bore x Stroke 3.78 x 3.19 (96 x 81)
 - Valve System SOHC, 24 valves, hydraulic, center-pivot roller rocker arms
 - Fuel Injection Sequential, multi-port, electronic
 - Construction Semi-permanent mold aluminum block with cast-in iron liners and cast aluminum heads
 - Compression Ratio 10.0:1
 - Power (SAE net) **250 HP bhp (186 kW) @ 6400 rpm** (71.4 bhp/liter)
 - Torque (SAE net) **250 lb.-ft. (339 Nom) @ 3950 rpm**
 - Max. Engine Speed 6800 rpm
- Fuel Requirement Unleaded mid-grade, 89 octane (R+M)/2 -preferred, unleaded regular, 87 octane (R+M)/2 - acceptable
- Oil Capacity 5 qt. (4.75 L) with dry filter
- Coolant Capacity 10.5 qt. (9.9 L)
- Emission Controls: Three-way catalytic converter, electronic EGR, and internal engine features. Meets Federal Tier 2, Bin 9A emissions requirements; marketed in California as an ULEV (Ultra-Low Emission Vehicle) under cleanest vehicle rules.
- Max. Gross Trailer Weight 3500 lbs. (1600 kg) Estimated EPA Fuel Economy 17/22 (MPG City/Hwy.)

Transaxle: four-speed

- Adaptive electronic control, electronically modulated converter clutch.

Gear Ratios

- 1st 2.84
- 2nd 1.57
- 3rd 1.00

- 4th 0.69
- Final Drive Ratio 4.28
- Overall Top Gear 2.95

All-wheel Drive

- Center Differential Viscous coupling
- Torque Split, F/R Variable: 0-90 percent
- Rear Differential Open

Electrical System

- Alternator 160 A
- Battery Group 34, maintenance-free: 500 CCA

Dimensions and Capacities (at curb weight)

- Wheelbase 116.3 (2954)
- Track, Front 66.0 (1676)
- Track, Rear 66.0 (1676)
- Overall Length 198.9 (5052)
- Overall Width 79.3 (2013)
- Overall Height 66.5 (1688)
- Cargo Floor Height 28.6 (726)
- Ground Clearance 5.9 (149)
- Curb Weight-est. 4675 lbs. (2121 kg) - AWD, 4482 lbs. (2033 kg) - initial FWD, 4393 lbs. (1993 kg) - lower-priced FWD
- Weight Distribution, % F/R 55/45 - AWD, 56/44 -FWD
- Frontal Area 30.55 sq. ft. (2.84 sq. m)
- Drag Coefficient 0.355
- Fuel Tank Capacity 23 gal. (87 L)

Accommodations

- Seating Capacity, F/I/R 2/2/2

Front

- Headroom (without sunroof) 39.2 (996)
- Legroom 40.9 (1040)
- Shoulder Room 60.8 (1545)
- Hip Room 55.1 (1401)
- Seat Travel 8.2 (208)
- Front Volume Index 56.2 cu. ft. (1.59 cu. m)

2nd Row

- Headroom 40.4 (1025)
- Legroom 38.9 (988)
- Knee Clearance 2.8 (72)
- Shoulder Room 60.5 (1538)
- Hip Room 56.3 (1430)
- 2nd Row Volume Index 55.0 cu. ft. (1.56 cu. m)

3rd Row

- Headroom 35.4 (900)
- Legroom 29.9 (760)
- Knee Clearance 0.1 (2)
- Shoulder Room 58.0 (1472)

- Hip Room 41.9 (1063)
- 3rd Row Volume Index 32.2 cu. ft. (0.91 cu. m)
- Front Volume Index 143.3 cu. ft. (4.06 cu. m)

Cargo Volume Indexes

- Aft of 2nd Row 43.6 cu. ft. (1.23 cu. m)
- Aft of 3rd Row 13.0 cu. ft. (369 L)
- All Seats Folded 79.5 cu. ft. (2.25 cu. m)

Body

- Transverse front engine, all-wheel drive or front-wheel drive
- Construction Unitized steel body with rubber-isolated front and rear suspension cradles, manual liftgate with temperature compensated gas props - std., power liftgate - opt.

Suspension

- Front: Iso struts with integral gas-charged shock absorbers, coil springs, asymmetrical lower control arms, link-type stabilizer bar and urethane jounce bumpers
- Rear: Five-link independent with coil springs, link-type stabilizer bar and gas-charged, self-levelling shock absorbers

Steering

- Type Rack and pinion, variable-assist droop-flow power
- Overall Ratio 17.8:1
- Turning Diameter (curb-to-curb) 39.8 ft. (12.1 m)
- Steering Turns (lock-to-lock) 3.18

Tires

- Michelin MXV4 Energy P235/65 R17 (others may be used)
Revs per Mile (km) 717 (445)

Wheels

- Cast aluminum 17 x 7.5

Brakes

- Front: 12.5 x 1.1 (318 x 28) vented disc with 1.88 (48) diameter two-piston sliding caliper
- Swept Area 291.1 sq. in. (1878.2 sq. cm)
- Rear: 12.25 x 0.55 (312 x 14) disc with 1.65 (42) diameter single-piston caliper
- Swept Area 189.3 sq. in. (1221.4 sq. cm)

Appendix B - Gapped Inductor Design for DC-DC Converter

Gapped Inductor Design Using Core Geometry Approach

Step 1 - Specifications

Total Inductance	$L_{eq} := 0.000025\text{H}$
Number of Parallel Inductors	$n := 4$
Inductance, L	$L := L_{eq} \cdot n = 1 \times 10^{-4}\text{H}$
Total DC Current	$I_{eq} := 1412\text{A}$
Per Inductor DC Current, I_0	$I_0 := \frac{I_{eq}}{n} = 353\text{A}$
Total Ripple Current	$I_{rip} := 40\text{A}$
Per Inductor AC Current, ΔI	$\Delta I := \frac{I_{rip}}{n} = 10\text{A}$
Total Output Power	$P_t := 1.5 \cdot 10^5\text{W}$
Output Power, P_0	$P_0 := \frac{P_t}{n} = 3.75 \times 10^4\text{W}$
Regulation, α	$\alpha := 1$
Ripple Frequency, f	$f := 200\text{kHz}$
Operating flux density, B_m	$B_m := 0.5\text{T}$
Core Material	Ferrite
Window Utilization, K_u	$K_u := 0.4$
Temperature rise goal, T_r	$T_r := 25^\circ\text{C}$

Step 2 - Peak Current

$$I_{pk} := I_0 + \frac{\Delta I}{2} = 358 \text{ A}$$

Step 3 - Energy Handling

$$E_h := \frac{L \cdot I_{pk}^2}{2} = 6.408 \text{ W} \cdot \text{s}$$

Step 4 - Electrical Conditions Coefficient

$$K_e := 0.145 \left(\frac{P_o}{W} \right) \cdot \left(\frac{B_m}{T} \right)^2 \cdot (10^{-4}) = 0.136$$

Step 5 - Core Geometry Coefficient

$$K_g := \frac{\left(\frac{E_h}{J} \right)^2}{K_e \cdot \alpha} \cdot \text{cm}^5 = 302.088 \text{ cm}^5$$

Step 6 - Select or Define Core

Core number	180UI
Magnetic Path Length	MPL := 50.29m
Core Weight	W _{tfe} := 7491gr
Mean Length Turn	MLT := 26.28m
Iron Area	A _c := 19.858m ²
Window Area	W _a := 52.258m ²
Area Product	A _p := 1037.74m ⁴
Core Geometry	K _g := 313.636m ⁵
Surface Area	A _t := 1296cm ²
Permeability	P := 2500μ _C
Milli Henrys per 1k turns	L ₁₀₀₀ := 3295mH
Winding Length	G _w := 11.43m
Total iron weight	n · W _{tfe} = 29.964kg

Step 7 - Current Density

$$J_d := \frac{2 \cdot \frac{E_h}{J} \cdot 10^4}{\frac{B_m}{T} \cdot \frac{A_p}{\text{cm}^4} \cdot K_u} \cdot \frac{A}{\text{cm}^2} = 617.515 \frac{A}{\text{cm}^2}$$

Step 8 - RMS Current

$$I_{\text{RMS}} := \sqrt{I_0^2 + \Delta I^2} = 353.142A$$

Step 9 - Required Bare Wire Area

$$A_{\text{wB}} := \frac{I_{\text{RMS}}}{J_d} = 0.572\text{cm}^2$$

Step 10 - Select Wire

2 strands of AWG #0

Max current 211A

Strands $\text{str} := 2$

Diameter $d := 8.2513\text{mm}$

Bare $A_{wB} := \text{str} \cdot \pi \cdot \left(\frac{d}{2}\right)^2 = 1.1\text{cm}^2$

Insulated $A_w := \text{str} \cdot 1.1 \cdot A_{wB} = 2.353\text{cm}^2$

Resistance $r := \frac{0.0983}{\text{str}} \cdot \frac{\Omega}{100\text{ft}} = 1.613 \times 10^{-4} \cdot \frac{\Omega}{\text{m}}$

Step 11 - Effective Window Area

$S_3 := 0.7$

$W_{\text{aef}} := W_a \cdot S_3 = 39.194\text{cm}^2$

Step 12 - Number of Turns Possible

$S_2 := 0.6$

$N := \frac{W_{\text{aef}} \cdot S_2}{A_w} = 9.995$

Step 13 - Required Gap Length

$$l_g := \left(\frac{0.4 \pi \cdot N^2 \cdot \frac{A_c}{\text{cm}^2} \cdot 10^{-8}}{\frac{L}{H}} - \frac{\frac{\text{MPL}}{\text{cm}}}{\mu_0} \right) \text{cm} = 0.229\text{cm}$$

Step 14 - Calculate Equivalent Gap in mils

$\text{mils} := l_g \cdot 393.7 = 90.225\text{cm}$

Step 15 - Fringing Flux Factor

$$F_r := 1 + \frac{\frac{l_g}{\text{cm}}}{\sqrt{\frac{A_c}{\text{cm}^2}}} \ln \left(\frac{2 \cdot \frac{G_w}{\text{cm}}}{\frac{l_g}{\text{cm}}} \right) = 1.237$$

Step 16 - New Number of Turns

$$N_{nn} := \sqrt{\frac{\frac{l_g}{\text{cm}} \cdot \frac{L}{\text{H}}}{0.4\pi \cdot \frac{A_c}{\text{cm}^2} \cdot F_r \cdot 10^{-8}}} = 8.617$$

$$N_n := \text{round}(N_{nn}) = 9$$

Step 17 - Winding Resistance

$$R_L := \text{MLT} \cdot N_n \cdot r = 3.814 \times 10^{-4} \Omega$$

Step 18 - Copper Loss

$$P_{\text{cu}} := I_{\text{RMS}}^2 \cdot R_L = 47.564 \text{W}$$

Step 19 - Regulation

$$\alpha := \frac{P_{\text{cu}}}{P_o} \cdot 100 = 0.127$$

Step 20 - AC Flux Density

$$B_{\text{ac}} := \frac{0.4\pi \cdot N_n \cdot F_r \cdot \left(\frac{\Delta I}{2 \cdot A} \right) \cdot 10^{-4}}{\frac{l_g}{\text{cm}} + \frac{\frac{\text{MPL}}{\text{cm}}}{\frac{P}{\mu_0}}} T = 0.028 \text{T}$$

Step 21 - Watts per Kilogram

$$k := 0.0000485 \quad m := 1.6 \quad n := 2.6$$

$$mWg := k \cdot \left(\frac{f}{\text{Hz}} \right)^m \cdot \left(\frac{B_{ac}}{T} \right)^n \frac{W}{\text{kg}} = 1.822 \frac{W}{\text{kg}}$$

Step 22 - Core Loss

$$P_{fe} := mWg \cdot W_{tfe} = 13.65W$$

Step 23 - Total Loss

$$P_{\Sigma} := P_{cu} + P_{fe} = 61.214W \quad \frac{P_o}{P_{\Sigma} + P_o} = 0.998$$

Step 24 - Watt Density

$$\Psi := \frac{P_{\Sigma}}{A_t} = 0.047 \frac{W}{\text{cm}^2}$$

Step 25 - Temperature Rise

$$T_{\Delta} := 450 \left(\frac{\Psi}{\frac{W}{\text{cm}^2}} \right)^{0.826} = 36.152$$

Step 26 - Peak Flux Density

$$B_{pk} := \frac{0.4\pi \cdot N_n \cdot F_r \cdot \left(\frac{I_0 + \frac{\Delta I}{2}}{A} \right) \cdot 10^{-4}}{\frac{l_g}{\text{cm}} + \frac{MPL \cdot \mu_0}{P \cdot \text{cm}}} \cdot T = 2.009T$$

Appendix C - Battery Discharge Model

Parameters for each of three cell types were estimated from their manufacturer's data sheets [REF] to mimic their discharge behaviour. The discharge profile for the high capacity cell as per its manufacturer datasheet is given together with the corresponding Matlab model discharge profile.

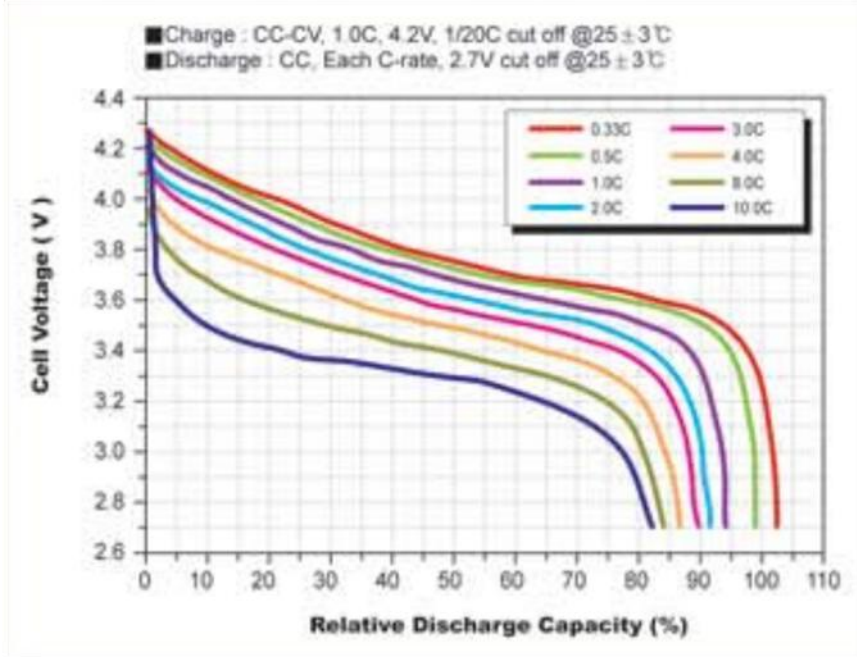


Figure I - High capacity battery discharge profile (datasheet)

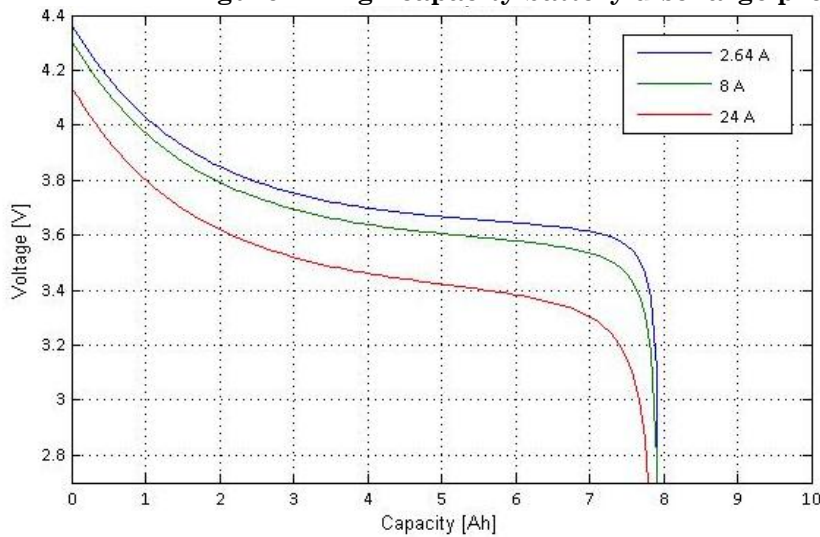


Figure II - High capacity battery discharge profile (Matlab model)

Appendix D - Battery and Capacitor Cell Parameters

This table shows details of the battery cells used herein [REF]. Referenced models are highlighted.

1. High energy density cell

Part #	Model	Capacity (Ah)	Dimension (mm)			Weight (g)	Max. Discharge Rate (C)		Energy Density (Wh / Kg)
			Thickness	Width	Height		Continuous	Pulse	
500001-0101A	SLPB 50106100	5	5.0 ± 0.2	106 ± 2.0	100 ± 2.0	115 ± 5.0	1	5	177
800001-0101A	SLPB 75106100	8	7.5 ± 0.3	106 ± 2.0	100 ± 2.0	155 ± 5.0	1	5	190
800001-0101A	SLPB 68106100	8	6.8 ± 0.3	106 ± 2.0	100 ± 2.0	150 ± 5.0	1	2	196
016K01-0101A	SLPB 75106205	16	7.5 ± 0.3	106 ± 2.0	205 ± 2.0	330 ± 10	1	2	180
025K01-0101A	SLPB 60216216	25	6.5 ± 0.3	215 ± 2.0	220 ± 2.0	620 ± 20	1	5	155
030K01-0101A	SLPB 68216216	30	6.8 ± 0.3	215 ± 2.0	220 ± 2.0	700 ± 20	1	5	156
040K01-0101A	SLPB 90216216	40	9.0 ± 0.5	215 ± 2.0	220 ± 2.0	935 ± 30	1	5	163
070K01-0101A	SLPB 53460330	70	5.3 ± 0.3	455 ± 2.0	325 ± 2.0	1700 ± 50	1	5	160
100K01-0101A	SLPB 70460330	100	7.2 ± 0.3	455 ± 2.0	325 ± 2.0	2320 ± 70	1	3	163
200K01-0101A	SLPB 140460330	200	14.0 ± 0.5	465 ± 2.0	340 ± 2.0	4400 ± 130	1	2	168

2. High power cell

Part #	Model	Capacity (Ah)	Dimension (mm)			Weight (g)	Max. Discharge Rate (C)		Energy Density (Wh / Kg)
			Thickness	Width	Height		Continuous	Pulse	
500005-0101A	SLPB 30205130H	5	3.1 ± 0.3	206 ± 2.0	130 ± 2.0	164 ± 6.0	5	10	113
750005-0101A	SLPB 41205130H	7.5	4.2 ± 0.3	206 ± 2.0	130 ± 2.0	226 ± 9.0	5	10	123
011K05-0101A	SLPB 55205130H	11	5.6 ± 0.3	206 ± 2.0	130 ± 2.0	292 ± 12	5	10	139
031K05-0101A	SLPB 78216216H	31	8.4 ± 0.5	215 ± 2.0	220 ± 2.0	860 ± 40	5	10	133
040K05-0101A	SLPB 100216216H	40	10.7 ± 0.5	215 ± 2.0	220 ± 2.0	1100 ± 40	5	10	135
070K05-0101A	SLPB 60460330H	70	5.8 ± 0.3	455 ± 2.0	325 ± 2.0	1950 ± 80	5	10	133
100K05-0101A	SLPB 80460330H	100	8.1 ± 0.3	455 ± 2.0	325 ± 2.0	2700 ± 100	5	8	137
200K02-0101A	SLPB 160460330H	200	17.0 ± 0.5	465 ± 2.0	340 ± 2.0	5260 ± 260	2	4	141

3. Ultra high power cell

Part #	Model	Capacity (Ah)	Dimension (mm)			Weight (g)	Max. Discharge Rate (C)		Peak Power Density (W / Kg)
			Thickness	Width	Height		Continuous	Pulse	
720005-0101A	SLPB 45205130P	7.2	4.5 ± 0.5	206 ± 2.0	130 ± 2.0	226 ± 10	5	20	2600
012K05-0101A	SLPB 70205130P	12	7.0 ± 0.5	206 ± 2.0	130 ± 2.0	354 ± 15	5	20	1850

This table shows details of the ultra capacitors used in this work [REF]. The referenced cell is highlighted.

Rated Capacitance	Internal Resistance (mΩ)		Max. Current (A)	Leakage Current (mA)	Stored Energy (Wh)	Specific Energy (Wh/kg)	Weight (g)	Part Number
	Discharge with constant current at 25°C	AC(100Hz)	DC	1 sec discharge rate to 1/2V _R	72hours, 25°C	at V _R		
600F	< 0.64	< 0.83	541	1.7	0.608	2.90	210	ESHSP-0600C0-002R7
1700F	< 0.50	< 0.65	1,090	2.4	1.721	4.47	385	ESHSP-1700C0-002R7
3500F	< 0.28	< 0.36	2,091	5.5	3.544	5.17	685	ESHSP-3500C0-002R7
5000F	< 0.25	< 0.33	2,547	8.1	5.063	5.44	930	ESHSP-5000C0-002R7

Rated Voltage, V _R	2.7 V	
Surge Voltage	2.85 V	
Capacitance Tolerance	0% / +20%	
Operating Temperature Range	-40 ~ 65 °C	ΔC <5% and ΔESR < 0.5 times of initially measured value at 25°C, respectively
Storage Temperature Range	-40 ~ 70 °C	
Life Time at RT ⁽¹⁾	10 years	(1) ΔC < 30% and ΔESR < 1 times of initially specified value , respectively and LC < specified value
Cycle Life (25°C) ⁽¹⁾⁽²⁾	500,000 cycles	(2) Cycle : between rated voltage and half rated voltage under constant current at 25°C

Appendix E - Energy Usage Graphs

These graphs show the energy usage breakdown for each scenario, for the LA92, HWYCOL, and NYCCCOL drive schedules.

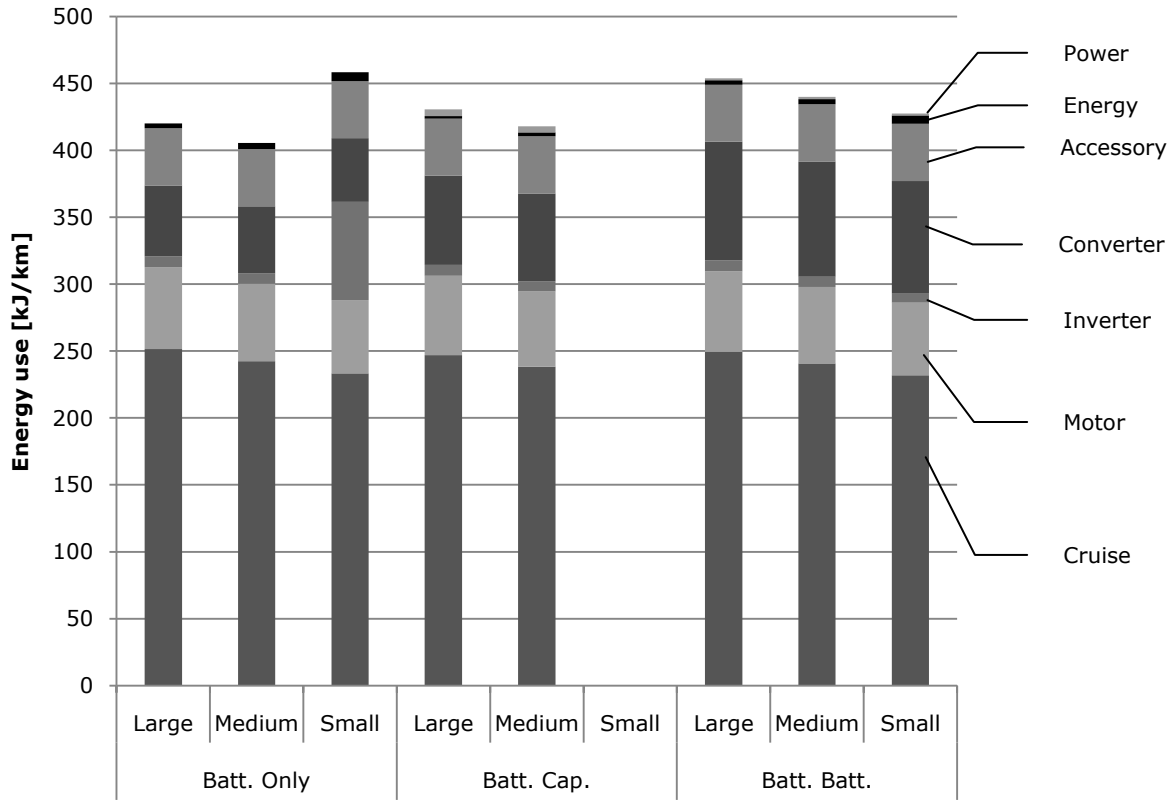


Figure III - Energy usage breakdown for LA92

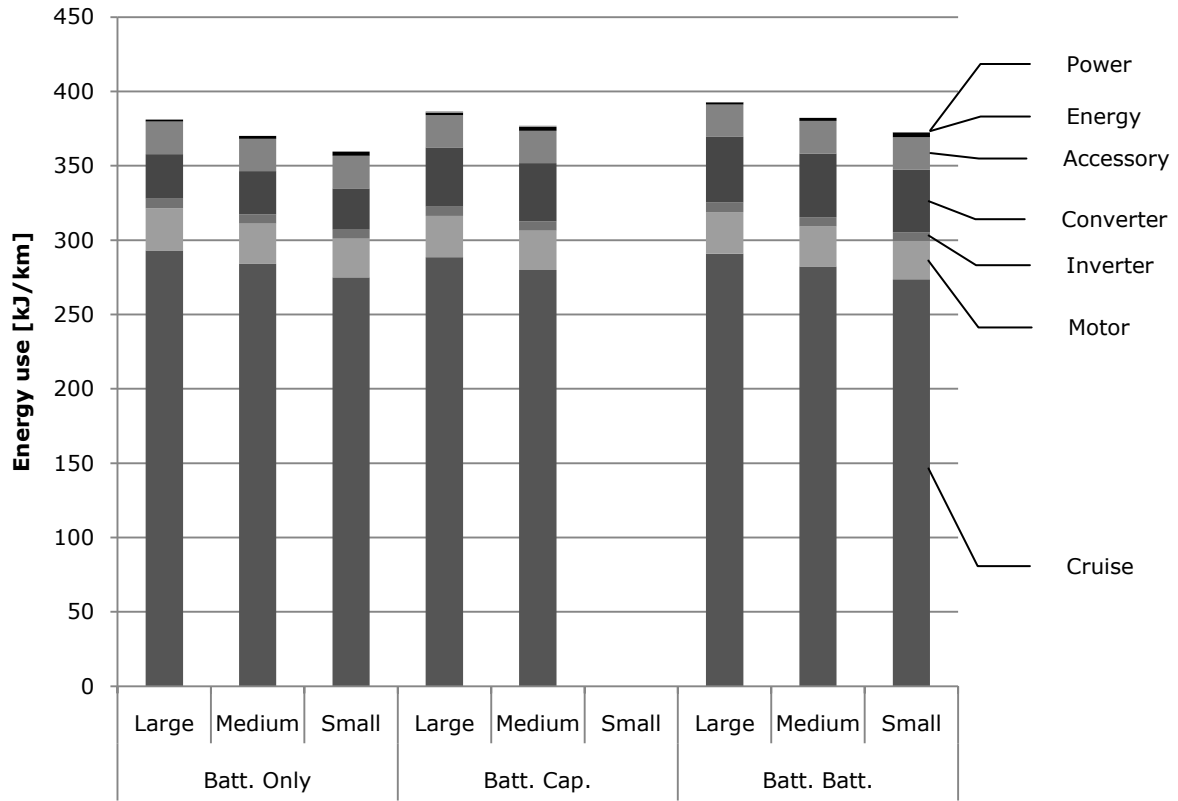


Figure IV - Energy usage breakdown for HWYCOL

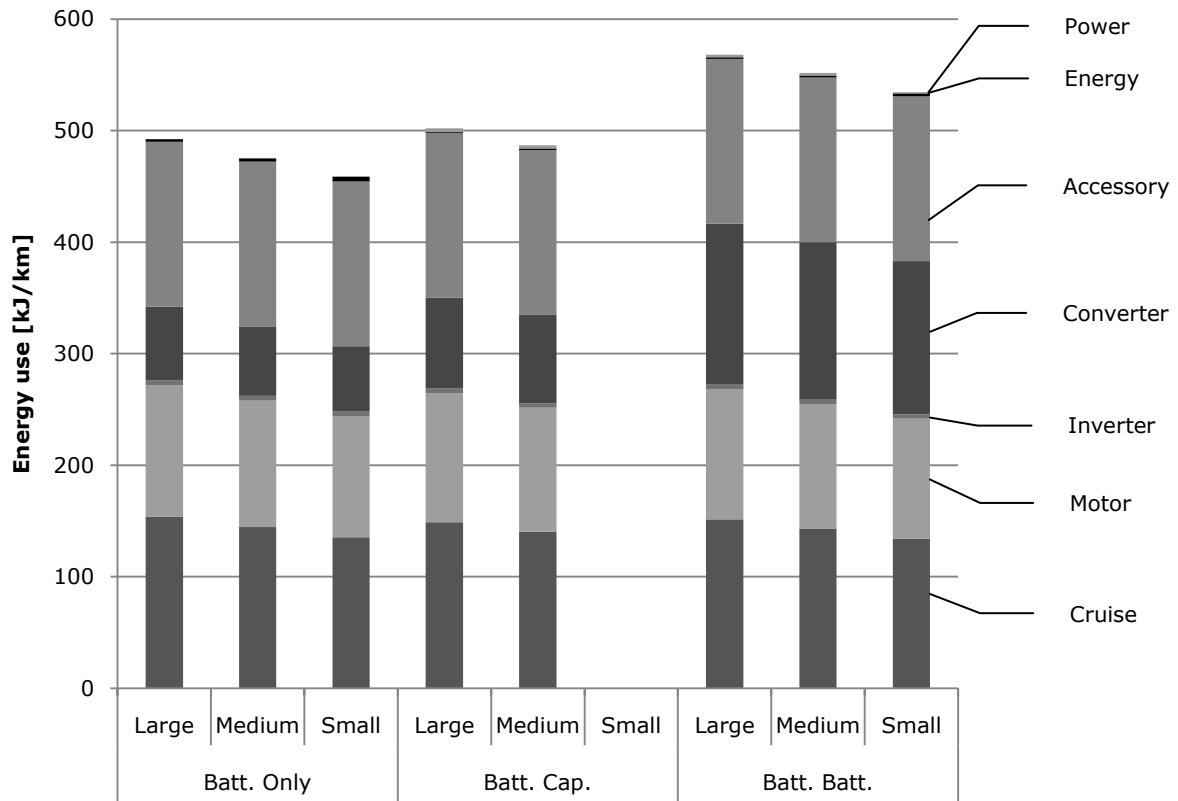


Figure V - Energy usage breakdown for NYCCOL

Appendix F - Demand Variation Graphs

These graphs show the demand variation for each scenario, for the LA92, HWYCOL, and NYCCCOL drive schedules.

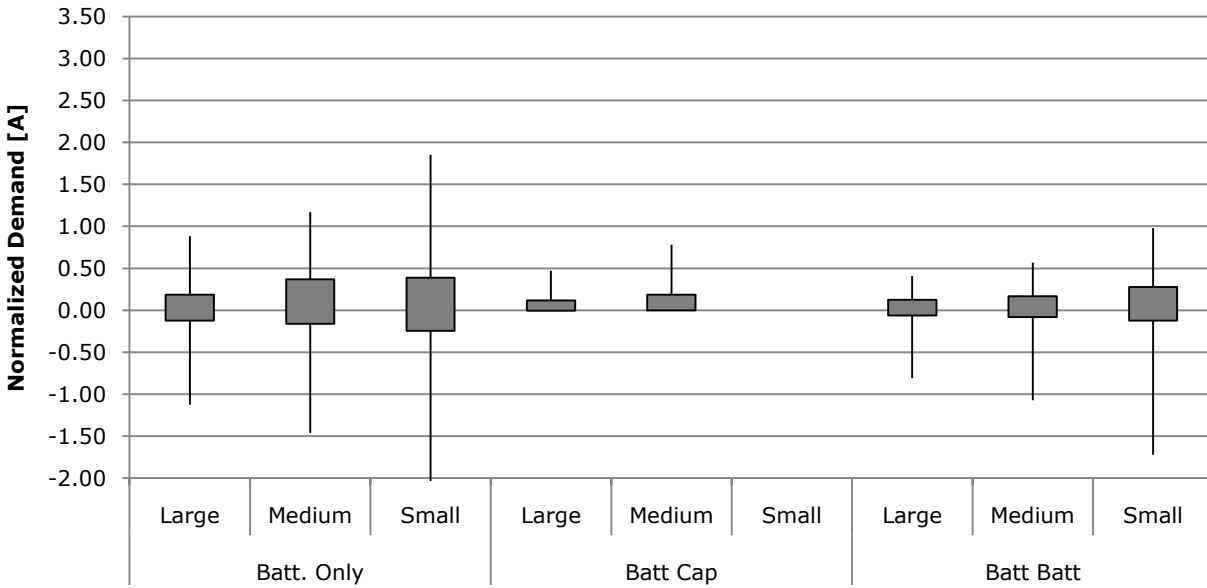


Figure VI - Demand variation for LA92

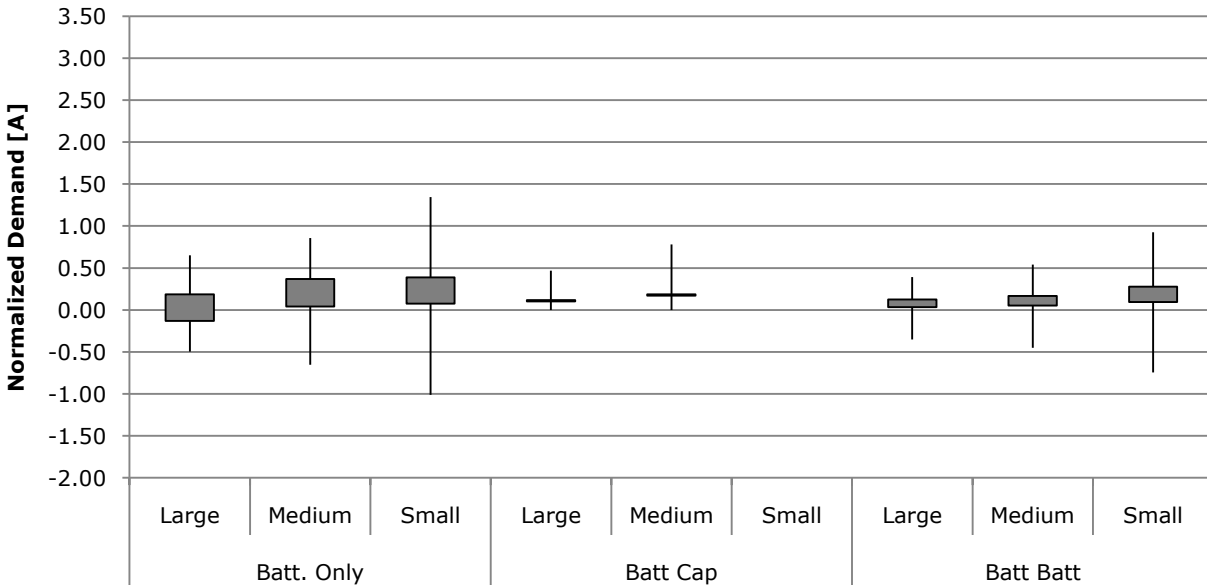


Figure VII - Demand variation for HWYCOL

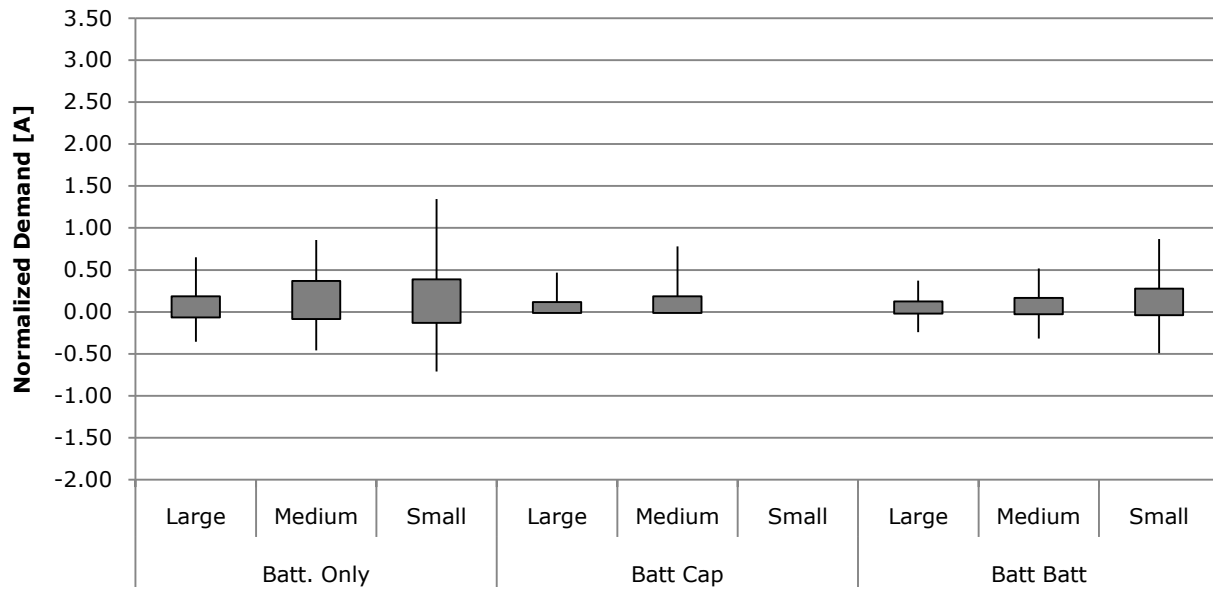


Figure VIII - Demand variation for NYCCOL